HYBRID PROPULSION TECHNOLOGY PROGRAM

Volume II
TECHNOLOGY DEFINITION PACKAGE

15 October 1989

Contract No. NAS 8-37778

Prepared by

G. E. Jensen
A. L. Holzman
S. O. Leisch
J. Keilbach
R. Parsley
J. Humphrey

Prepared for

GEORGE C. MARSHALL SPACE FLIGHT CENTER
NATIONAL AERONAUTICS AND SPACE ADMINISTRATION
MARSHALL SPACE FLIGHT CENTER, AL 35812

by

UNITED TECHNOLOGIES CHEMICAL SYSTEMS

P.O. Box 49028
San Jose, CA 95161-9028

CONTENTS

ILLUSTRATIONS

TABLES

TABLES (CONTINUED)

1.0 INTRODUCTION

The recommended technology definition program provides for acquisition and subscale demonstration of the hybrid propulsion technologies needed to enable application of hybrid propulsion to manned and unmanned space launch vehicles.

Formulation of the technology definition program began with an assessment of the recommended hybrid motor systems concepts to identify technology development needs. The four recommended concepts presented in Figure 1-1 are the 4.57-m (180-in.) design with fuel No. 7 (all hydrocarbon), the 3.96-m (156-in.) design with fuel No. 8 (partially oxidized), and the 2.44-m (96-in.) quarter-scale design with fuel No. 7 used either with separate oxidizer tanks or as a quad combustor to provide single chamber shutdown capability. The technology development needs of these four concepts are identified in Table 1-1. These concepts cover a wide range of candidate configurations for large hybrid boosters.

Technology development needs are focused on the hybrid combustion chamber and the key interfaces with the oxidizer supply. All other technologies required for a large hybrid booster are sufficiently common to existing large solid and liquid boosters to be excluded from consideration on this program. With the exception of the relative significance of LOX injection, fuel ignition and fuel development for the partially oxidized (fuel No. 8) concept, all four concepts require the complete spectrum of hybrid technologies with about the same priority from one concept to another. Therefore motor concept selection is not a significant discriminator in formulating the hybrid technology definition program.

Formulation of the recommended technology definition program followed the logical path outlined in Figure 1-2. Each of these steps is presented and discussed in the indicated sections of this plan. The motor concepts were used to identify candidate technology development areas. Each of the identified technologies was evaluated to define shortcomings that justify technology development for large hybrid booster application. Ranking criteria were

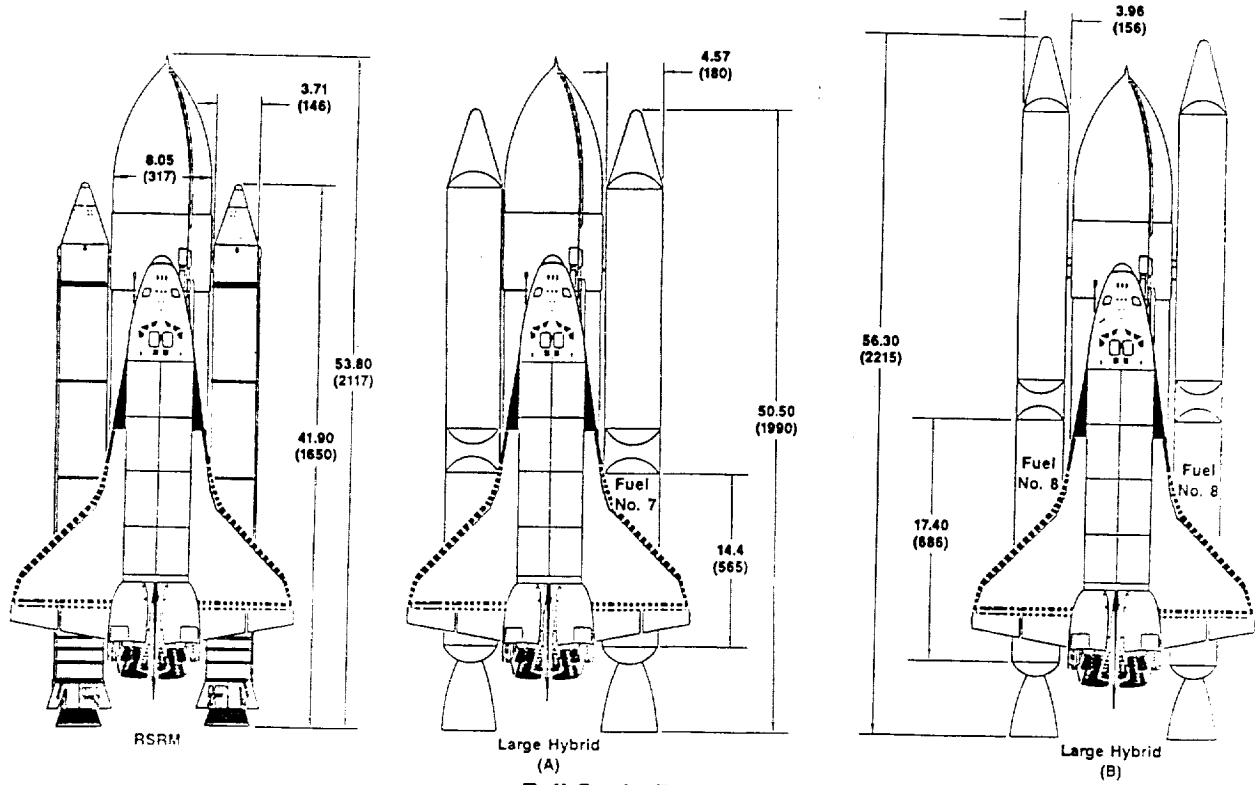

Figure 1-1. Recommended (R) Motor System Concepts

50483

TABLE 1-1. HYBRID PROPULSION TECHNOLOGY IDENTIFICATION - RECOMMENDED CONCEPT ASSESSMENT

T16992

Recommended Motor Concepts	Technology Development Areas						
	LOX Injection	Ignition System	Fuel Development	Fuel Grain	Insulation	Nozzle	Consumable Mandrels
Full-scale boosters 4.5m (180 in.), Fuel No. 7	X	X	✓	X	✓	X	✓
3.96m (156 in.), Fuel No. 8	✓	✓	X	X	✓	X	✓
2.44m (96 in.) - quad fuel No. 7	X	X	✓	X	✓	X	✓
2.44m (96 in.) - 1/4-scale, fuel No. 7	X	X	✓	X	✓	X	✓

Note: X = major development area; ✓ = moderate development area

Summary: Motor concept selection is not a significant discriminator in most technology development areas. The AP loading in fuel No. 8 reduces the significance of injector/igniter development and increases the significance of fuel development.

developed and justified as a basis for quantifying the relative development importance of each of the identified technologies. The ranking criteria were then used to assess each identified technology and develop a priority rank. Technology acquisition plans were prepared for each identified technology. These plans included schedules and technology acquisition costs. Finally, a large subscale motor demonstration plan was developed using existing 3.05-m (120-in.) Titan hardware. The recommended technology acquisition/demonstration efforts will advance the maturity of hybrid propulsion technology to a level sufficient for application to future manned and unmanned space launch vehicles.

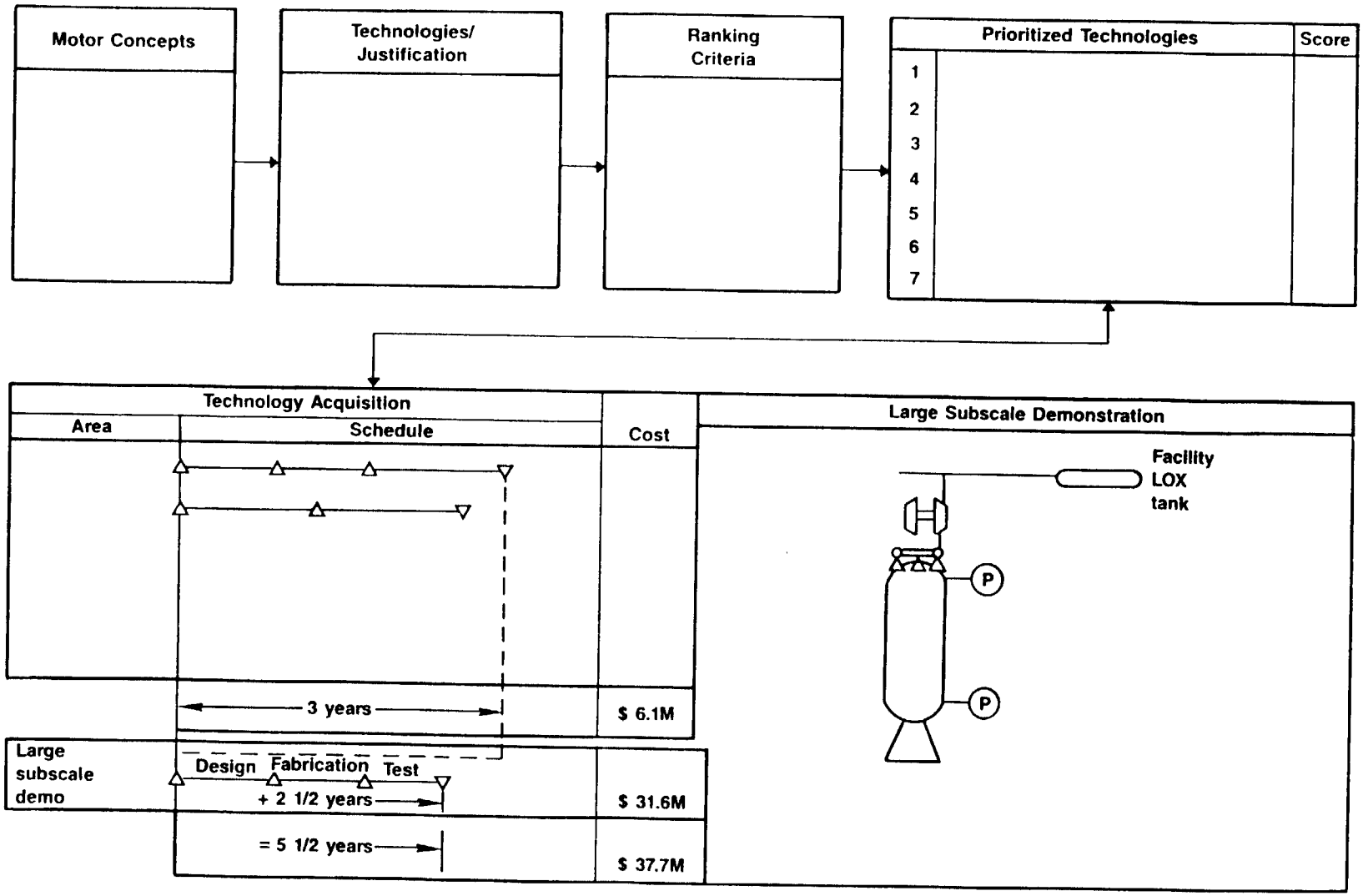

Figure 1-2. Technology Definition Plan Outline

50453

2.0 TECHNOLOGY IDENTIFICATION

The hybrid technologies required to enable the development of the recommended hybrid propulsion concepts are identified, justified and ranked by priority in this section. The technologies were screened to focus development resources on technologies unique to hybrid rocket motors. The shortcomings of existing hybrid motor technology for large booster applications were evaluated in each of the identified technology areas. This assessment is summarized in Table 2-1.

Most of the shortcomings of existing technology relate to the size effects required to apply hybrid propulsion to very large motors and to differences in design approaches or material selection for large motors. The oxidizer feed system is a key linking technology between the oxidizer tank and the hybrid combustion chamber. LOX pump feed systems are a mature technology that requires no development on this program. Pressure-fed LOX system technology will be obtained in other programs. However, use of a gaseous oxygen pump would require technology development to define coupled motor pump interaction effects and to advance the GOX pump technology to a sufficient level of maturity for full-scale development (FSD). Fuel development is required to develop structural, ballistic and processing characteristics that are optimum for large hybrid fuel grains. Fuel grain development is needed to develop grains which have the required fuel flow characteristics while achieving minimum residual fuel and high combustion efficiency. Consumable mandrel technology offers an approach to facilitate fuel grain development and processing. Oxidizer injector development is coupled to the fuel grain development to achieve uniform fuel regression and handle the range of oxidizer mass fluxes required for large hybrid boosters. Ignition system development is needed to handle the relatively complex fuel grains required for large hybrid boosters and to ensure repeatable ignition for potential multiple booster applications.

Large boosters offer opportunities for the use of low-cost insulation materials and fabrication techniques in the nozzle and case insulation. In some cases their large size actually precludes the use of technology developed

TABLE 2-1. TECHNOLOGY SHORTCOMINGS ASSESSMENT

T17028

Identified Technology Development Area	SOA Shortcoming Relative to Large Booster Application
Oxidizer feed system LOX GOX	• Mature technology; no development needed or in progress • Coupled operation of motor and GOX pump, materials compatibility, proof of concept
Fuel development	• Optimum formulation for large fuel grains; regression characteristic, physical properties
Fuel grain design and ballistics	• Size effects relative to fuel ballistics and combustion efficiency
Injection system	• Size effects relative to achieving uniform fuel regression oxidizer mass flux limits and quality of oxygen
Ignition system	• Size and grain complexity effects on hybrid ignition
Nozzle	• Size/low cost material effects
Insulation	• Size/low cost material effects
TVC	• Erosion effects on exit cone, performance
Control requirements	• Need hybrid chamber response, multipump operation and TVC impact.

for smaller systems. These two factors combine to favor technology development of nozzle and internal case insulation materials. The promising use of LOX LITVC in large hybrid boosters requires confirmation of the side specific impulse of LOX and evaluation of nozzle erosion effects with LOX injection.

The ranking criteria shown in Table 2-2 were developed to evaluate the relative importance of the identified technology development activities. Five criteria were used including three technical criteria together with development lead time and development cost. Each technology was evaluated against these criteria on a scale of 1 to 10. The sum of these values provides an

TABLE 2-2. HYBRID TECHNOLOGY RANKING CRITERIA

T16993

Ranking Criteria	Description
Design significance	Technical • How significant are technology development objectives to the successful use of this component on the recommended motor concepts?
Technical risk	• What is the technical risk of failure to meet technology development program objectives for this component?
Available alternatives	• Are acceptable alternative design approaches available if the technology program does not develop the recommended aproach?
Development lead time	Schedule • How does the technology program schedule for this component compare with the critical path schedule?
Development cost	Cost • How does the technology development program cost for this component compare with the technology development costs for other components?

overall quantification of the urgency of devoting resources to that activity. An identified technology needs to be significant to the successful use of the subject component on the recommended concepts. Development priority is increased if the technology has a higher-than-average technical risk. The availability of acceptable alternate design approaches reduces the urgency for technology development. A long development lead time increases the priority of technology development. Development cost has both positive and negative implications. From a pure technology acquisition standpoint, cost is not an incentive. However, for a program aimed at demonstrating all the technologies required for a complete hybrid motor system, more expensive technologies represent greater program risk and were given high development priority. In summary, a high-priority technology is significant to the design (i.e., requires technology development to meet component requirements), has significant technical risk, has no readily available design alternates, and requires both significant development time and money.

The identified technology areas were evaluated and scored against the ranking criteria. The results of the individual technology assessments are presented in Tables 2-3 through 2-9 and summarized in Table 2-10.

The following technologies have been determined to be hybrid-specific areas of concern that require further development prior to demonstration testing.

TABLE 2-3. TECHNOLOGY DEVELOPMENT JUSTIFICATION - GRAIN DESIGN AND BALLISTICS
T16994

Development Scope: Develop a fuel grain using the selected fuel formulation and injector/oxidizer flow rate which provide the desired fuel flow rate history with minimum sliver. Develop/improve analytical models describing grain ballistics.

Evaluation Criteria	Discussion	Importance (Scale 1 to 10)
Design significance	Essential design element	10
Technical risk	Moderate risk associated with repeatable uniform axial and circumferential fuel regression	7
Available alternatives	None; must meet ballistic requirements	9
Development lead time	Significant effort due to fuel formulation/injector design coupling and size scaling effects	9
Development cost		7
	Total	42

Justification Summary: Most important hybrid motor development area

TABLE 2-4. TECHNOLOGY DEVELOPMENT JUSTIFICATION - FUEL DEVELOPMENT

T16995

Development Scope: Formulate fuel with desired structural/ballistic/ processing characteristics		
Evaluation Criteria	**Discussion**	**Importance (Scale 1 to 10)**
Design significance	Essential design element to hybrid booster	10
Technical risk	Low risk; apply technology to hybrid booster	5
Available alternatives	None; must have fuel that meets requirements	9
Development lead time	Relatively short development, but critical path element	9
Development cost	Moderate cost	4
	Total	37
Justification Summary: Although low risk, fuel development is a critical path development effort		

2.1 FUEL DEVELOPMENT

Fuel development, presented in Table 2-4, was given the second highest score of 37. The objective of fuel development technology is to formulate a fuel with the desired mechanical, ballistic and processing characteristics for large hybrid booster applications. While fuel development is considered to have low technical risk and moderate cost impact, the activity leads the fuel grain development and is therefore a critical path technology.

2.2 FUEL GRAIN DESIGN AND BALLISTICS

Fuel grain development, presented in Table 2-3, was given the highest motor technology development priority, with an overall score of 42. The objective of fuel grain technology is to develop a fuel grain that meets

TABLE 2-5. TECHNOLOGY DEVELOPMENT JUSTIFICATION - OXIDIZER INJECTION SYSTEM
T16996

Development Scope: Develop injection system that achieves desired hybrid ballistics with selected fuel/grain		
Evaluation Criteria	**Discussion**	**Importance (Scale 1 to 10)**
Design significance	Important element in hybrid ballistics	9
Technical risk	Moderate risk due to relatively high GOX_{max}	7
Available alternatives	Several approaches available	5
Development lead time	Must be developed concurrently with grain	9
Development cost	Moderate cost item	5
	Total	35
Justification Summary: Important, moderate risk design element that needs to be developed concurrently with the grain		

ballistic requirements with minimum residual fuel. Fuel grain development is essential to the design since there are no design alternatives. Lead time is relatively long due to the coupled interactions with the fuel formulation and injector technology efforts and the need to verify ballistic scaling effects. Technical risk and cost are considered moderate based on similar successful efforts on previous hybrid development programs.

2.2.1 Analytical Grain Regression Modeling

A review of the literature was conducted to identify and assess existing computational models potentially applicable in the prediction of the effects on hybrid grain regression rates of liquid components in the core flow within the grain port(s). Included in this review, which is discussed in detail in

TABLE 2-6. TECHNOLOGY DEVELOPMENT JUSTIFICATION - NOZZLE

T16997

Development Scope: Develop nozzle design/materials that meet motor performance requirements		
Evaluation Criteria	**Discussion**	**Importance (Scale 1 to 10)**
Design significance	Important design element	9
Technical risk	Moderate; large throat diameter facilitates longer chamber residence time and permits medium throat erosion	5
Available alternatives	Several candidate materials available	4
Development lead time	Use of LITVC reduces nozzle schedule/cost. Nozzle design/materials developed concurrently with grain	4
Development cost		5
	Total	31
Justification Summary: Important design element, moderate risk area		

Appendix A, were papers covering such topics as hybrid rockets, hybrid or heterogeneous combustion, solid-fueled rockets, and solid-fueled ramjets.[13-35] Papers about combustion in solid-fueled rockets and ramjets and about combustion instability in rockets were examined only to the extent that modeling approaches applicable to hybrid rockets might be derivable from such analyses. Information was also obtained from Acurex Corporation regarding the approaches used there for analyzing flows within the hybrid rocket combustor.

The available models can be divided into two general groups. In the first group, the regression rate is determined from one-dimensional analyses that assume that the flow conditions at the grain boundary are known or can be

TABLE 2-7. TECHNOLOGY DEVELOPMENT JUSTIFICATION - IGNITION SYSTEM

T16998

Development Scope: Develop a system to reliably achieve ignition in all parts of a multi-port grain		
Evaluation Criteria	**Discussion**	**Importance (Scale 1 to 10)**
Design significance	Important design requirement	9
Technical risk	Relatively low technical risk	4
Available alternatives	Several approaches available	5
Development lead time	Moderate development schedule/cost requirements	5
Development cost		4
	Total	27
Justification Summary: Important design element, but development can be delayed until injector/fuel/grain design technologies have been further defined		

estimated from other simple analyses or data. In the second group, computational fluid dynamics (CFD) methods are used to obtain important details of the flow field which are used as boundary conditions for models describing the chemical processes within the grain. In the latter category, no hybrid rocket analyses have been published. However, the applicability of CFD as a design tool for hybrid rockets is implicit in the observation that such analyses are now regularly used in modeling of a variety of complex combustion systems.

Although no papers on hybrid combustion modeling have been published in recent years, the basic understanding developed approximately 20 years ago is still largely applicable to anticipated motor designs. Hence, the models

TABLE 2-8. TECHNOLOGY DEVELOPMENT JUSTIFICATION - INSULATION

T16999

Development Scope: Develop case insulation for areas unprotected by fuel (primarily in the aft closure)

Evaluation Criteria	Discussion	Importance (Scale 1 to 10)
Design significance	Important design element	8
Technical risk	Low; similar requirements to those for solid motor insulation	4
Available alternatives	Several candidate materials available	4
Development lead time	Can be evaluated concurrently with fuel grain development tests	3
Development cost		3
	Total	22

Justification Summary: Lower priority development item

developed previously are still usable. For example, for the portion of the flow field far enough from the oxidizer injector that flow recirculation is unimportant and, in the case of a liquid oxidizer, the droplet number density is small enough, methods are available for predicting motor ballistic behavior. Indeed, such methods were employed in the present program as a basis for thrust chamber design calculations. Furthermore, models exist for extending these venerable one-dimensional analyses to include consideration of the effects of the presence of a liquid phase in the core flow. However, in the regions proximate to a liquid oxidizer injector, the flow field can be analyzed only by state-of-the-art CFD techniques.

In general, the flow within a hybrid rocket grain port is three-dimensional and consists of at least two distinct phases, the gas phase

TABLE 2-9. TECHNOLOGY DEVELOPMENT JUSTIFICATION - CONSUMABLE MANDREL MATERIALS

T17000

Development Scope: Develop consumable mandrels for use in grain casting (mandrels remain in motor)		
Evaluation Criteria	**Discussion**	**Importance (Scale 1 to 10)**
Design significance	Important design element	8
Technical risk	Relatively low technical risk	4
Available alternatives	Several candidate materials available	4
Development lead time	Can be evaluated concurrently with fuel grain development tests	2
Development cost	Relatively low cost item	2
	Total	20
Justification Summary: Lower priority development item		

together with liquid droplets or particles from the grain. For realistic engine geometries the flow field is three-dimensional and coupled thermodynamically to processes occurring within the grain. For low port mass fluxes, this coupling is weak in the sense that the regression rate is essentially a property of the solid fuel and is determined primarily by the local temperature within the grain. For higher flow rates, the coupling becomes stronger in the sense that the burning (regression) rate is controlled directly by the rates of heat and/or oxidizer mass transfer to the surface. These transfer rates, in turn, are affected by the rate of mass and energy transfer between the solid grain and the core flow. Hence, the general model of hybrid combustion is physically quite complex. However, it can be simplified greatly if suitable approximations can be made. If it can be assumed that the oxidizer

TABLE 2-10. TECHNOLOGY DEVELOPMENT RANKING

T17001

Technology Candidate	Evaluation Criteria Significance						
	Priority Rank	Design Significance	Technical Risk	Available Alternatives	Development Lead Time	Cost	Total
Fuel grain design and ballistics	1	10	7	9	9	7	42
Fuel development	2	10	5	9	9	4	37
Oxidizer injection system	3	9	7	5	9	5	35
Nozzle	4	9	6	6	5	5	27
Ignition system	4	9	4	5	5	4	27
Insulation	6	8	4	4	3	3	22
Control Technology	7	8	4	6	2	1	21
Consumable mandrels	7	8	4	4	2	2	20

will be injected as a gas or that the primary region of interest is far enough removed from the oxidizer injection station that the two-phase flow is essentially axial, then a multi-phase, multi-dimensional hybrid rocket engine model can be developed readily from the models already developed for solid rocket motors. Furthermore, for two-dimensional geometries, such CFD models can be operated conveniently and efficiently using modern computer work-stations. For three-dimensional flows, so-called mini supercomputers are adequate. Such codes can be exercised readily by non-specialist users.

The model for the region of the flow field in which the flow is essentially axial can be developed from the reduced form of the Navier-Stokes equations in which the streamwise "diffusion" terms have been omitted. For the hybrid rocket combustor, additional specifications are possible that permit the so-called boundary layer form of the governing equations to be obtained. Examples of the use of this equation set for modeling solid rocket motors are described in references 29 through 33. A space-marching solution method has also been used.[34] Since the work in reference 29 was conducted under Air Force sponsorship, it may prove possible to obtain a copy of such a code to be used as the basis for a computer program applicable to hybrid rocket motors. Note that the effects of a liquid phase in a hybrid rocket can be incorporated readily into the model. Generally, for axially directed, three-dimensional flows, a space-marching method can be used to obtain the secondary flows in the cross plane. With this detailed information, the local regression rates can be obtained at an instant of time. Using a separate, but straightforward, computer code and assuming that the local regression rate distribution remains unchanged for a specified time interval, a new port geometry can be obtained and a new regression rate distribution computed. In this manner, the flow and time-history within complex port geometries can be modeled.

For the head-end of the hybrid combustor, especially when liquid injection is used, the flow field can be (at best) analyzed using relatively sophisticated CFD codes. At present, such codes are best run by specialists using supercomputers. Since improved methods applicable to this portion of the flow field are being developed for other purposes, it is recommended that no unique additional development effort be made as part of a hybrid rocket development program. Developers and users of such codes are generally aware of current developments in the area. Some efforts are sponsored as part of the National Aerospace Plane program and other U. S. Government-sponsored activities. Technical papers describing new developments and applications of state-of-the-art CFD codes are presented at such meetings as the AIAA Aerospace Sciences meeting. Monitoring of progress in this area is anticipated as part of the Phase 2 program.

2.3 INJECTORS

Oxidizer injection system development, presented in Table 2-5, received a score of 35. The oxidizer injection system is closely coupled to the fuel grain design. The objective of the injection system technology is to achieve spatially uniform fuel regression over the required oxidizer mass flux range, not cause grain extinguishment, and promote high combustion efficiency. The injection system technology is essential to meeting fuel grain ballistic requirements and entails moderate technical risk due to the relatively high maximum oxidizer mass flux. However, there are several injector approaches that minimize program risk. A detailed discussion of the alternatives and why further work is required in this area is presented in Appendix B.

2.4 IGNITION SYSTEM

The ignition system, presented in Table 2-7, received a score of 31. The objective of the ignition technology is to achieve reliable ignition throughout a large multi-port hybrid grain. While ignition is deemed to have low technical risk, the coupling of the ignition system and the fuel grain/ injection system requires this technology to be defined early in the development program. Based on previous development programs there are several ignition system approaches available (see section 3.0).

2.5 INSULATION

Insulation development, presented in Table 2-8, received a score of 25. The objective of the insulation technology work is to develop an insulation material/process to insulate the exposed areas of the combustion chamber primarily in the aft and forward closures. Although the chamber insulation is an important design element, the similarity of hybrid motor and solid motor insulators reduces the importance of early efforts focused on insulation development.

2.6 MANDREL MATERIALS

Consumable mandrel development, presented in Table 2-9, received a score of 20. The objective of consumable mandrel technology is to facilitate the processing and ballistic characteristics of large hybrid fuel grains. The

ability to tailor the axial web thickness profile is particularly attractive in terms of optimizing the grain design and minimizing fuel sliver. This technology entails moderate development risk and lead time due to its limited development experience.

2.7 NOZZLE MATERIALS

Nozzle development, presented in Table 2-6, received a score of 31. The objective of the nozzle technology is to develop materials and a design that meet large hybrid booster performance requirements. The nozzle design is important in achieving good combustion efficiency by promoting recirculation in the aft closure. The selected nozzle materials must be appropriate for the environment to achieve a high reliability design. The large throat size facilitates a long chamber residence time to promote combustion efficiency and permits a relatively high throat erosion rate. Both these effects reduce the technical risk of nozzle development. Use of LOX LITVC simplifies the nozzle design, but requires a more erosion-resistant material in the exit cone.

2.8 SYSTEMS CONTROL TECHNOLOGY

Coordination of the oxidizer delivery, thrust chamber, and thrust vector control systems in a hybrid booster is required to obtain the full benefits of hybrid motor controllability. While analogous statements pertain to liquid and solid rockets, there is a uniqueness to hybrids that requires special attention in the controls area. This section presents descriptions of control system design issues that are particular to hybrid boosters. An assessment of control system design was performed for each of the two hybrid motor sizes that CSD identified as baselines for the present program, namely, a large hybrid duplicating the ASRM vacuum thrust-time profile and a smaller hybrid with 1/4-ASRM thrust level. Two types of oxidizer delivery system -- pump-fed and pressure-fed -- and two concepts for TVC -- gimbaled nozzle and liquid injection -- were considered in the analysis. Throughout the analysis, attention was directed to the facts that:

- The hybrid booster control system would be responsible for a number of actions, including motor start-up, shutdown, propellant tank pressurization, and safety monitoring and maintenance.
- Multiple pumping systems must be coordinated to achieve the global system oxidizer delivery requirements for pump-fed systems.
- Health maintenance logic must be developed for oxidizer delivery pumps which provides an indication when a single-pump shutdown is advisable.
- Control logic must be developed for pump-fed systems to facilitate a smooth transition from nominal operation to a single pump-out condition while maintaining engine thrust.
- Liquid injection TVC must be coordinated with the thrust chamber pressure control logic on systems utilizing LOX from the oxidizer delivery system for TVC injectant.
- The feedback control of motor chamber pressure requires a feedback loop to be closed around the thrust chamber dynamics, a non-stationary process.

Because development of logic to support specific control functions is very hardware-dependent, such was not the focus of this preliminary assessment. Rather, the main objectives of the present effort were concept formulation and identification of unresolved issues associated with the development of logic for control of the magnitude and direction of the hybrid-booster-motor-produced thrust.

2.9 OTHER CONCERNS

The alternative TVC concept, LITVC, is an established technology. The primary unknowns relative to large hybrid application are the side specific impulse of LOX and the erosion effects of LOX injection on the selected nozzle exit cone material. While confirmation of these effects during Phase 2 is desirable, this technology work could be deferred until FSD.

LOX injection using either tank pressurization or a warm, fuel-rich, gas turbine-driven pump is state-of-the-art technology that requires no development efforts during Phase 2 or 3. However selection of the GOX feed system

introduces a strong technology development requirement due to the lack of maturity of the GOX turbopump system and the design coupling of this system with the motor. Therefore technology development considerations favor a LOX pressurization system that does not require early development and does not compete with the key hybrid motor technology development efforts for funding. The necessity for using GOX injection has not been established and this issue will be addressed during Phase 2.

2.10 RANKING

The technology development ranking is summarized in Table 2-10. The core hybrid motor technologies of fuel development, fuel grain and oxidizer injection have the highest priority for technology resources. These coupled technologies are critical path items and need to be defined early. Ignition system and nozzle development are the technologies with the next highest priority. Insulation, TVC and consumable mandrel efforts are useful technologies that can be pursued if technology funding permits. A LOX oxidizer feed system would not require technology development funding and it is recommended to focus limited resources on essential hybrid motor technologies.

3.0 TECHNOLOGY ACQUISITION PLAN

The technologies identified in section 2.0 will be acquired according to the plan outlined in the following paragraphs. Many of the technology acquisition efiorts will be performed in an integrated manner, that is, several components will be developed and tested as part of the same test series. Nevertheless, each technology development area is discussed in a separate subsection, and cost estimates and schedule are presented at the end of section 3.0 for each identified technology.

An overview of the Phase 2 program is presented in Figure 3-1. The program begins with an update to the system studies of Phase 1 and fuel development work. These efforts are followed by several series of tests to evaluate and characterize each of the major technologies previously identified. A summary of these test series is presented in Table 3-1. Combustion testing will be performed in sizes ranging from laboratory-scale grains (0.064-m (2.5-in.) OD) and samples, to 1.22-m (48-in.) diameter motors. After the completion of testing in this phase, a preliminary assessment of hardware and test sites for Phase 3 will be conducted and included in the final report. This assessment will include an update of cost and schedule estimates.

3.1 SYSTEM STUDY UPDATE

The initial portion of Phase 2 will require an update to the system studies conducted under the current phase. Since the intentional absence of a specific mission in Phase 1 precluded the establishment of precise design requirements, design concepts have been established instead. Prior to acquiring any of the technologies identified in section 2.0, the specific design requirements must be defined so that appropriate decisions and technology selections can be made relative to the major components. For example, several fuel formulations were presented as potential candidates for the hybrid booster. In order to select one or two fuels to carry through the Phase 2 development and test effort, specific requirements as to regression rate, density, pressure sensitivity, etc. must be defined. Similar arguments apply to the grain design and material selections for the nozzle, insulation, etc.

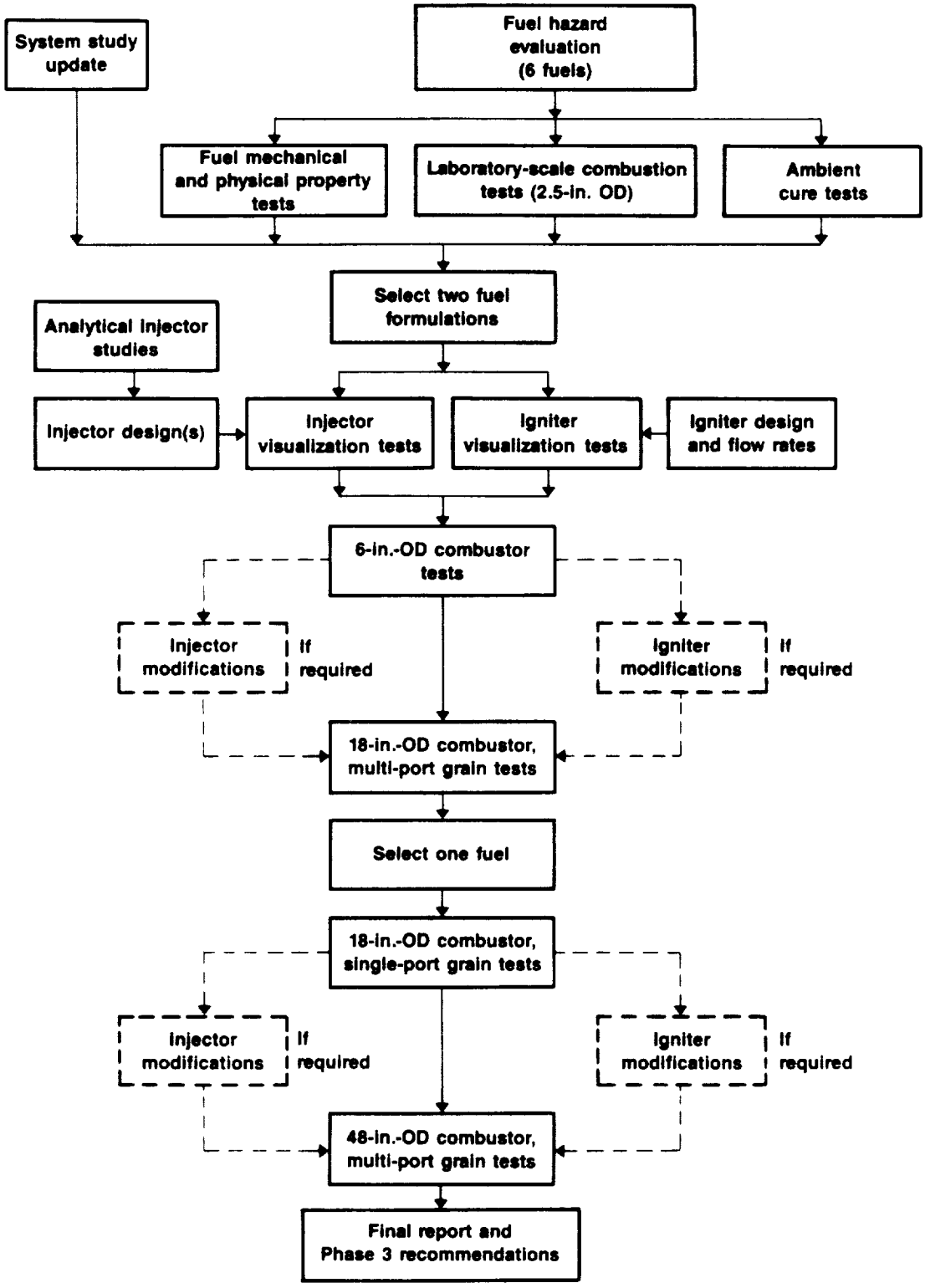

Figure 3-1. Phase 2 Program Flow Diagram

50454

TABLE 3-1. SUMMARY OF PHASE 2 TEST SERIES
(Sheet 1 of 2)

T17002

1. Fuel hazard evaluation
   - 6 fuels (vary oxidizer content of one formulation)
   - Burn rate tests
   - Thermal stability (autoignition temperature)
   - Impact
   - Friction
   - ESD

2. Laboratory-scale, 0.064-m (2.5-in.) OD combustion tests
   - 4 fuels
   - Single-port grains
   - GOX feed
   - Effect of $(L/D_h)_{port}$ and ozidizer mass flux on regression rate and combustion efficiency

3. Fuel mechanical and physical properties
   - 4 fuels
   - Uniaxial stress and strain
   - Biaxial stress and strain
   - Bond-in-tension stress
   - Constant stress endurance
   - Density
   - Coefficient of thermal expansion
   - Thermal conductivity

Based on tests 1 to 3, select 2 fuel formulations for further study.

4. Slab burner tests
   - Evaluate spray vaporization and impingement
   - Evaluate regression rate

5. Combustion tests with 0.15-m (6-in.) OD grains
   - 1 fuel, single-port grains
   - Evaluate LOX and GOX injection
   - Evaluate ignition system variables
   - Evaluate injector configurations
   - Evaluate nozzle materials
   - Evaluate insulation materials
   - Evaluate consumable mandrel material(s)
   - Evaluate effects of fuel grain cracks/voids
   - Evaluate scaling laws
   - Evaluate port geometry effects
   - Evaluate effects of pressure and port L/D_h

TABLE 3-1. SUMMARY OF PHASE 2 TEST SERIES
(Sheet 2 of 2)

T17002

6. Combustion tests with 0.46-m (18-in.) OD grains
   - 1 fuel, multi-port grains, same port size as in No. 5
   - Evaluate multi-port effects (fuel utilization, $\dot{r}$, etc.)
   - Evaluate injector configurations
   - Evaluate ignition system variables
   - Evaluate throttling capability
   - Evaluate grain retention system(s)
   - Evaluate effects of fuel grain cracks/voids
   - Evaluate additional materials

7. Combustion tests with 0.46-m (18-in.) OD grains
   - 1 fuel, single-port
   - Evaluate scaling laws (G, P, L/D)
   - Evaluate igniter fuel flow rate requirements
   - Evaluate throttling capability
   - Evaluate fuel utilization
   - Evaluate repeatability ($\dot{r}$, combustion efficiency, etc.)

8. Combustion tests with 1.22-m (48-in.) OD grains
   - 1 fuel, multi-port, same port size as in No. 6
   - Optimize igniter fuel flow rate
   - Verify/optimize injector configuration
   - Evaluate throttling capability
   - Evaluate fuel utilization
   - Evaluate structural integrity of grain design
   - Evaluate repeatability

The specific mission requirements will therefore be defined at the outset of the Phase 2 program through mutual agreement by NASA and United Technologies/CSD. This will be followed by a system study update in which the mission requirements will be inputted to the design code and specific motor design goals and requirements will be established through use of the code. These motor design results will be used to make selections among the recommended options for the major hybrid components.

3.2 FUEL DEVELOPMENT

The primary motivation for developing a hybrid booster is increased flight safety. One of the keys to attaining this increased safety is having a solid fuel that is insensitive to stimuli such as friction, electrostatic

discharge (ESD), grain cracking, etc., and does not deflagrate without the presence of an oxidizer. The first step in the fuel development effort will therefore be to establish the hazard characteristics of six fuel formulations containing various amounts of solid oxidizer. Oxidizer levels from 0 to 30% will be formulated and tested. A summary of the hazard tests to be performed is given in Table 3-2.

Following hazard characterization, four fuel formulations will be selected for small-scale ballistic tests and mechanical property testing. The current plan is to test formulation numbers 1, 5, 7, and 8 as identified in Volume I of this report; however, this selection will depend on the outcome of the hazard testing. A summary of the laboratory-scale testing is presented in Table 3-3. Standard circular port grains (see Figure 3-2) will be tested with gaseous oxygen (GOX) to establish the effects of oxidizer mass flux and fuel port L/D on regression rate and combustion efficiency. This data will be used later to select two fuels before proceeding to a larger scale fuel grain.

TABLE 3-2. PHASE 2 - FUEL HAZARD EVALUATION

T17004

Test Description	Objective
Thermal stability	Autoignition temperature (ambient pressure)
Impact	Energy density to initiate reaction
Friction	Force/unit area at a given velocity to initiate reaction
ESD	Spark energy required to initiate reaction
Burn rate	Determine if fuels are self-sustaining at various pressures

Note: Hazard evaluation tests will be conducted with fuel Nos. 1, 5, 7, 8, and variations of fuel No. 8 with different oxidizer contents.

TABLE 3-3. PHASE 2 - LABORATORY-SCALE COMBUSTION TEST SERIES (0.064-M (2.5-IN.) OD, SINGLE-PORT)

T17005

Test No.	Fuel No.	Port L/D_h	G_{O2}, kg/s-m^2 (lb/sec-in.^{2})	Objective
1	1	25	351.5 (0.5)	Baseline condition - fuel No. 1
2	1	25	210.9 (0.3)	Effect of lower G_{O2} on regression rate
3	1	25	70.3 (0.1)	Effect of lower G_{O2} on regression rate
4	1	40	351.5 (0.5)	Effect of increased L/D_h on regression rate
5	1	40	70.3 (0.1)	Effect of lower G_{O2} on regression rate
6	5	25	1054.6 (1.5)	Baseline condition - fuel No. 5
7	5	25	632.8 (0.9)	Effect of lower G_{O2} on regression rate
8	5	25	210.9 (0.3)	Effect of lower G_{O2} on regression rate
9	5	40	1054.6 (1.5)	Effect of increased L/D_h on regression rate
10	5	40	210.9 (0.3)	Effect of lower G_{O2} on regression rate
11	7	25	562.5 (0.8)	Same as above
12	7	25	351.5 (0.5)	
13	7	25	140.6 (0.2)	
14	7	40	562.5 (0.8)	
15	7	40	140.6 (0.2)	
16	8	25	1265.5 (1.8)	Same as above
17	8	25	773.4 (1.1)	
18	8	25	281.2 (0.4)	
19	8	40	1265.5 (1.8)	
20	8	40	281.2 (0.4)	

Instrumentation: aft grain pressure (P_4), thrust (F), oxygen feed pressure (P_{O2}), oxygen feed temperature (T_{O2}), regression rate (posttest or continuous, r)

Mechanical and physical property testing will also be performed with the four selected formulations mentioned above. A summary of these tests is presented in Table 3-4. These values will be required to support subsequent structural and thermal analyses of the selected booster design.

As discussed in Volume I of this report, reduction of thermally induced grain stress can be achieved by curing the grain at a temperature equal or

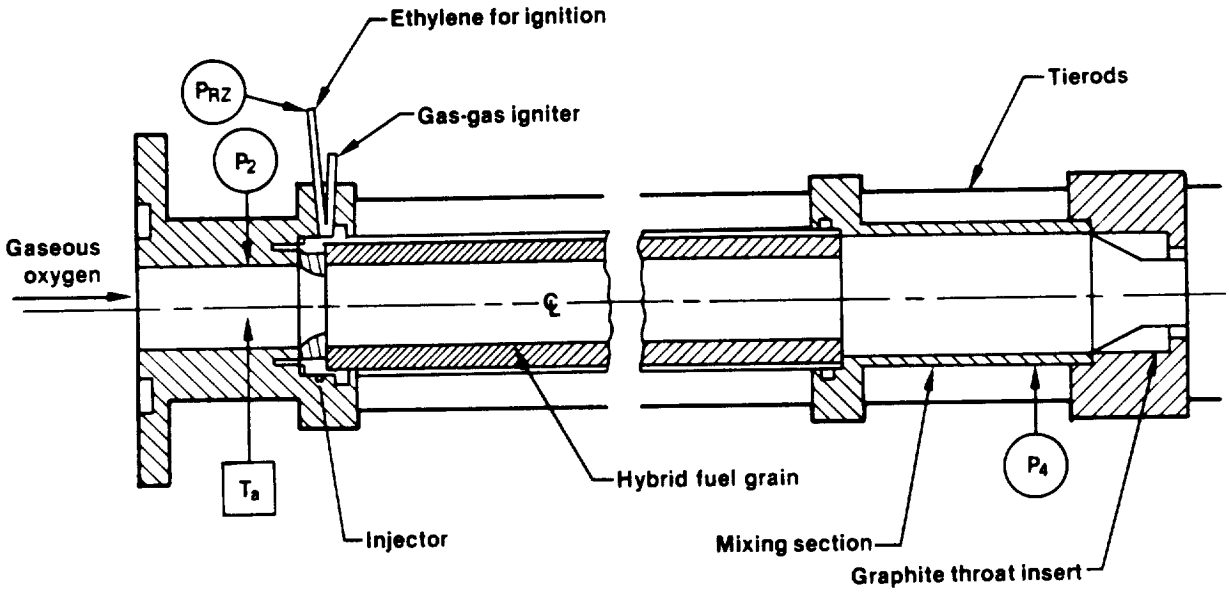

Note:
P_{RZ} = recirculation zone pressure, P_2 = inlet pressure, T_a = inlet total air temperature, P_4 = chamber pressure

Figure 3-2. Laboratory-Scale (0.064-m (2.5-in.) Diameter) Hybrid Combustor Design

44343

TABLE 3-4. PHASE 2 - FUEL MECHANICAL AND PHYSICAL PROPERTIES

T17006

Test	Objective
Uniaxial constant rate	Maximum stress and strain capability as a function of sample temperature
Biaxial tension	Biaxial stress and strain capabilities
Constant rate bond-in-tension	Bond-in-tension stress capability
Constant stress endurance	Constant stress capability as a function of time
Density	Self-explanatory
Coefficient of thermal expansion	Self-explanatory
Thermal conductivity	Self-explanatory

close to ambient. Cure studies have been performed at CSD with propellants at reduced temperatures from the standard 333 K (140°F). These techniques have not been applied to hybrid fuels and therefore a small effort will be undertaken to develop a technique applicable to hybrid grains. This study will consist of casting several strain evaluation cylinders and mechanical property cartons at 5.6 K (10°F) intervals from ambient to 333 K (140°F) for each candidate curative. Two or more curatives will be selected for this study. After the specified cure time has elapsed, the cylinders will be cycled over the required temperature operating range and the associated strain will be measured. The cartons of fuel will be used to prepare samples for mechanical property testing at various temperatures. Results of this test series will be used to establish if low temperature curing is appropriate for the hybrid booster.

3.3 FUEL GRAIN BALLISTICS

3.3.1 Analytical Grain Regression Rate Modeling

The state-of-the-art in modeling flows similar to those found in the hybrid rocket combustor (e.g., flows in gas turbine combustors or diesel engine combustion chambers) entails application of three-dimensional CFD codes. Existing three-dimensional Navier-Stokes analyses should be applied to model the flow field in the head end of hybrid rocket motors. Codes such as KIVA[26] are available from U. S. Government agencies. Relatively simple modifications are required to include the effects of heat and mass transfer between the grain and main flow in the boundary conditions for the main flow solver. For motors where the oxidizer is injected as a liquid, it will be necessary to assume the liquid behaves as a dilute spray. (In a dilute spray the droplet number density is large enough to be statistically significant (that is, there can be substantial exchanges of mass, momentum and energy between phases), but the volume fraction of the liquid is small.) Furthermore, the initial state of the spray must be specified; the spray formation process is not treated, because rigorous analysis of dense-spray effects is beyond the state-of-the-art. Hence, results obtained from Navier-Stokes for the liquid injection case will be somewhat less accurate than for the gas-injection case.

Downstream of the head end, the flow in the rocket motor is essentially axial. Based on results from solid-fueled rocket and ramjet applications (e.g., references 29 through 33), it is apparent that space-marching methods can be developed for computing the three-dimensional flow within the port. It is recommended that such analyses be developed, perhaps from a code developed previously for modeling solid-fueled motors.

The burning rate models and information necessary for regression model calibration should be developed from slab-burning test results. It is unnecessary to conduct tests in which complex physical processes are present within complicated geometries. (In elaborate tests, it is often impossible to obtain sufficient information on flow boundary and initial conditions.)

3.3.2 Experimental Slab Burner Studies

The efficacy of improved spray vaporization, impingement and grain regression rate models should be evaluated in a series of slab burner tests. These tests would be conducted in a specially fabricated test section in the high-pressure rocket combustion test facility of the UTRC Jet Burner Test Stand (JBTS). During these tests, fuel grain slabs of selected composition would be burned in a two-dimensional windowed reactor at various pressures with "core" flows having various spray patterns, mass fluxes and compositions.

The slab burner test section used in this program would be designed and fabricated as a two-dimensional, heat-sink-type model. It would incorporate an interchangeable upstream section for the mounting of various injector configurations for the controlled variation of the oxidizer spray pattern and interchangeable nozzles for the adjustment of reactor pressure. The fuel slabs would be located on the lower wall. Numerous pairs of opposed sidewall windows would be mounted in the test section for optical access and the fields of view would include the fuel slab surface as well as the regions upstream and downstream of the slab. Windows would also be included in the top wall of the test section to provide orthogonal optical access for advanced diagnostic techniques requiring intersecting beams. The test section would also include

a blank plate that could be substituted for the fuel slab in those tests conducted to characterize the injector spray pattern in the absence of combustion.

The UTRC high-pressure rocket combustion facility comprises a liquid oxygen supply and feed system; gaseous oxygen and nitrogen supply and feed systems; a test stand, including integral high-pressure water cooling and exhaust systems; a rocket control system; and a high-speed data acquisition system. The LOX system consists of a 1.89-m^3 (500-gal) low-pressure (0.69-MPa (100-psi)) storage Dewar and a 0.076-m^3 (20-gal) high-pressure (17.2-MPa (2500-psi)) insulated run tank. Both tanks are protected by fire barriers and blast walls. The LOX tank is pressurized with either high-pressure nitrogen or oxygen and is operated in a blowdown mode. The rocket test stand is enclosed in an explosion-proof cell, and is suitable for firing rocket motors operating at thrust levels up to 11,120 N (2500 lb). Rocket exhaust gases are expelled to the atmosphere through an ejector-pumped exhaust duct. Water for cooling selected components and exhaust ducts and for sup-pression of noise is supplied at high flow rates and pressures up to 13.8 MPa (2000 psi). A fully automatic, programmable electrical control system is used to provide accurate time-sequencing and recording of all rocket motor operations, and to incorporate fail-safe provisions that prevent loss of control of the rocket during operation. Timing of control system events would be fully adjustable, providing for flexibility of test run programming.

A test matrix for the recommended slab burner tests is presented in Table 3-5. The tests would begin with a characterization of the oxidizer flow field created by each of three candidate injector element configurations in the slab burner test section in the absence of combustion. Then, for each of the three injector element configurations, a parametric series of five tests would be conducted with a baseline fuel grain slab, covering controlled ranges of oxidizer flow rate and reactor pressure. On completion of those tests, two injector configurations would be selected and tested over a similar matrix but with fuel grain slabs having a different composition. During each test, overall regression rates would be determined by measuring fuel grain weight

TABLE 3-5. SLAB BURNER TEST MATRIX

T17029

Test No.	Injector Configuration	Grain Composition	Oxidizer Flow rate	Reactor Pressure
1	I1	None	W1	P1
2	I1	None	W2	P2
3	I2	None	W1	P1
4	I2	None	W2	P2
5	I3	None	W1	P1
6	I3	None	W2	P2
7	I1	G1	W1	P1
8	I1	G1	W2	P1
9	I1	G1	W3	P1
10	I1	G1	W2	P2
11	I1	G1	W2	P3
12 to 16	I2	G1	Repeat tests 7 to 11	
17 to 21	I3	G1	Repeat tests 7 to 11	
22 to 26	Selected A	G2	Repeat tests 7 to 11	
27 to 31	Selected B	G2	Repeat tests 7 to 11	

changes, while more detailed local surface regression rates would be determined as functions of distance along the surface using direct high-speed photographic techniques. Various available optical and thermometry techniques (as discussed in Appendix D) would also be applied, as appropriate, to effect spatial mapping of temperature, velocity and species concentration in the core flow boundary layer. The detailed database established as a result of these tests would be used in combination with the results of the spray modeling analysis to support the formulation and calibration of an improved model of the hybrid grain regression process. In particular, the ability of the analytical model to predict the observed parametric trends would be confirmed.

3.3.3 Connected-Pipe Testing

Following the laboratory-scale tests for fuel development and basic injection techniques, a series of connected-pipe tests in hardware varying

from 0.15-m (6.0-in.) to 1.22-m (48-in.) diameter will be conducted. This will be done in a systematic approach as shown in Figure 3-3. Initial tests will be conducted with 0.15-m (6-in.) diameter, single-port grains to investigate the basic effects of oxidizer mass flux, port L/D, combustor pressure, as well as to integrate the testing of the other major components. This series will be followed by 0.46-m (18-in.) OD combustor tests with multi-port grains. The area of each port will be kept the same as in the tests with single-port grains (0.15 m (6 in.)). The port size will then be scaled up and tested in basically the same 0.46-m (18-in.) hardware. The final connected-pipe tests will be conducted in 1.22-m (48-in.) diameter hardware and multi-port grains.

The first connected-pipe test series will be performed with single-port grains duplicating the shape of the full-scale design but being subscale in

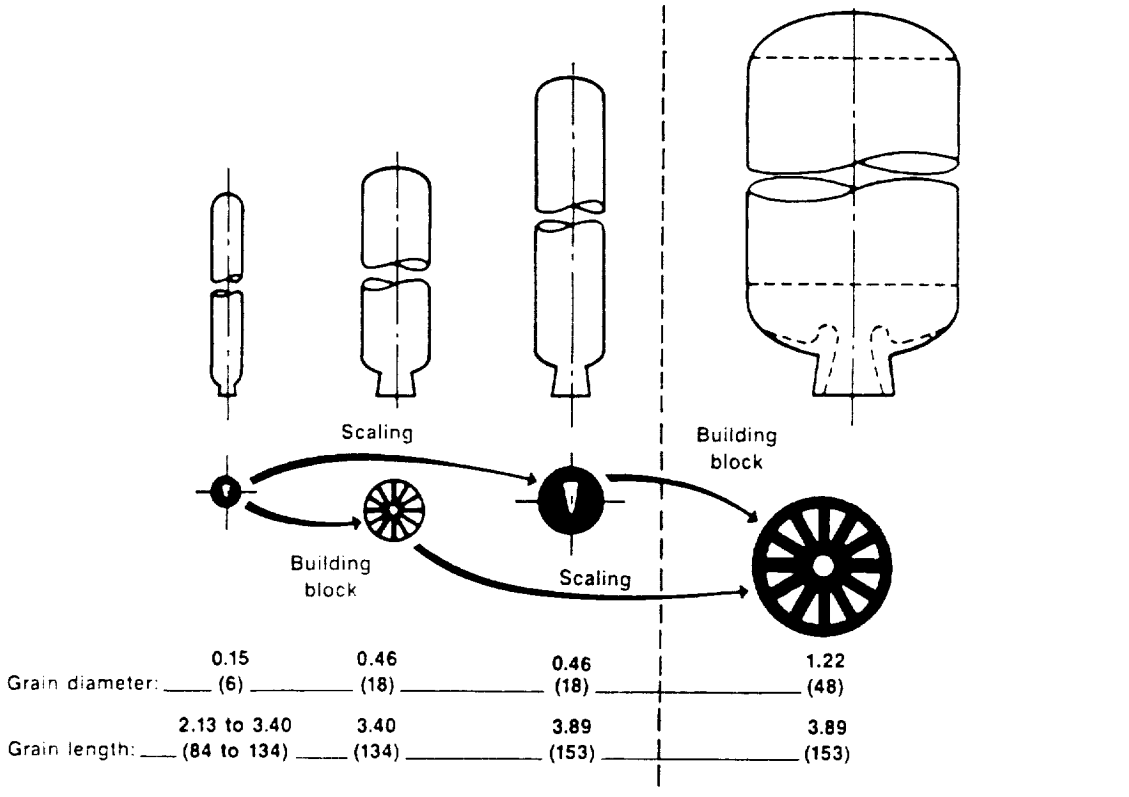

Note: All dimensions are in meters (inches)

Figure 3-3. Scaling Methodology for Phase 2

46319

size. The grains will include a head-end dome region as present in the full-scale design. During this test series the effects of injector configuration, pressure, oxidizer mass flux, and oxidizer phase (liquid or gaseous or a mixture of each) on regression rate, combustion efficiency, and fuel utilization will be evaluated. The effects of grain L/D_h ratio will also be evaluated using a minimum of two grain lengths. In addition, variations in igniter operating conditions such as igniter fuel flow rate and oxidizer ramp-up time will be evaluated and an optimum set of conditions selected for the remainder of the series. This test series will also be used as a means to evaluate several insulation, nozzle, and consumable mandrel materials under actual hybrid motor operating conditions. Finally, the effect of cracks and/or voids will be verified through the intentional creation of such defects and observation of the results. A photograph of a 0.15-m (6-in.) hybrid motor on the thrust stand is shown in Figure 3-4. This is one of several stands available at CSD for hybrid motor testing.

A minimum series of 20 tests is planned for this series; however, the start/stop capability of the hybrid allows additional tests to be conducted at relatively modest cost. Contingency tests can therefore be conducted to optimize injector or ignition configurations, if necessary. A summary of the planned tests is presented in Table 3-6. These tests would be performed in the CSD 1810 test facility, which has the capability of either gaseous or liquid oxygen injection.

Some configuration and test parameters have been identified for this test series and are summarized in Table 3-7. Port scaling from the booster designs results in a port area of 5.68×10^{-3} m^2 (8.8 $in.^2$). It is desirable to test with a port L/D_h equal to the booster designs so that a grain length yielding a 40:1 length to area ratio has been indicated. The effect of L/D_h will be evaluated with a second value of 25. Another important similarity parameter is the oxidizer flux rate through the port(s). In order to keep this equivalent to the booster design, a maximum oxidizer flow rate of 3.4 kg/s (7.5 lb/sec) will be required. By holding these design parameters constant, the resulting fuel flow rate will be such that the operating mixture

C18077-22 **Figure 3-4. CSD 0.15-m (6-in.) Diameter Hybrid Test Stand** 44422

ratio will closely match that of the booster motor. Assuming an I_{sp} of 303 sec (fuel No. 7), a maximum thrust of 13,900 N (3125 lb) will result. Each grain will contain approximately 42.2 kg (93 lb) of fuel.

Instrumentation required for the 0.15-m (6-in.) OD test series includes combustor pressure (P_4), thrust (F), head-end dome pressure (P_3), oxygen supply pressure (P_{02}), oxygen supply temperature (T_{02}), oxidizer flow rate, and regression rate (ultrasonic). This test series will be conducted at CSD on its RT-6 stand.

The scale of combustion tests will next be increased to 0.46-m (18-in.) OD. These tests will be performed with multiport grains having the same size

TABLE 3-6. COMBUSTION TEST SERIES WITH 0.15-m (6-in.) OD GRAINS

Part 1

T17007

Test No.	G_{O2}	$\dot{W}_{ign}$	Injector Configuration	Insulation Materials Tested	Nozzle Materials Tested	LOX or GOX	Comment/Objective
1	X*	$(0.03)\cdot X\cdot A_p$	1	None	Carbon-phenolic	GOX	Baseline/evaluate ignition response
2	X	$(0.04)\cdot X\cdot A_p$†	1	None	Carbon-phenolic	GOX	Evaluate effect of igniter fuel flow rate
3	X	$(0.05)\cdot X\cdot A_p$†	1	EPDM/Kevlar	Carbon-phenolic	GOX	Evaluate effect of igniter fuel flow rate
4	X	Optimum	2	Trowelable EPDM	Carbon-phenolic	LOX	Effect of injector/material testing
5	X	Optimum	3	HTPB/carbon	Silica-phenolic	LOX	Effect of injector/material testing
6	X	Optimum	Optimum	PE fiber/ epoxy resin mandrel	Silica-phenolic	Optimum	Evaluate regression rate of consumable mandrel material
7	X/5	Optimum	Optimum	EPDM/Kevlar	Carbon-phenolic	Optimum	Evaluate material at lower G_{O2}
8	X/5	Optimum	Optimum	Trowelable EPDM	Carbon-phenolic	Optimum	Evaluate material at lower G_{O2}
9	X/5	Optimum	Optimum	HTPB/carbon	Silica-phenolic	Optimum	Evaluate material at lower G_{O2}
10	X	Optimum	Optimum	EPDM/Kevlar	Silica-phenolic	Optimum	Evaluate effect of fuel grain cracks

* Value based on fuel selection
† Value may be modified based on results of test No. 1

Note: Initial L/D_h = 40; tests 1 to 10 conducted with throat size corresponding to 5.17 MPa (750 psia) at maximum flow rate

Instrumentation: P_4, P_3, F, P_{O2}, T_{O2}, $\dot{r}$

Part 2

T17038

Test No.	G_{O2}	$(L/D_h)_{port}$	Chamber Pressure, MPa (psia)†
11	X/2*	25	1.72 (250)
12	X/2	25	3.45 (500)
13	X/2	25	5.17 (750)
14	X/2	40	1.72 (250)
15	X/2	40	3.45 (500)
16	X/2	40	5.17 (750)
17	X	40	3.45 (500)
18	X/3	40	3.45 (500)
19	X/4	40	3.45 (500)
20	X/4	40	1.72 (250)

* Value based on fuel selection
† Value obtained by different nozzle throat sizes

TABLE 3-7. CONFIGURATION SUMMARY FOR 0.15-M (6-IN.) OD COMBUSTOR TESTS
T17027

Parameter	Value
Motor case diameter, m (in.)	0.15 (6)
Grain length, m (in.) (2)	2.13 (84); 3.40 (134)
No. of ports	1
Total port area, m^2 ($in.^2$)	5.68×10^{-3} (8.8)
Port L/D_h (2)	25; 40
Maximum thrust, N (lb)	13,900 (3125)
Maximum O_2 flow rate, kg/s (lb/sec)	3.41 (7.5)
Fuel weight, kg (lb)	42.2 (93)
Pressure, MPa (psia)	1.72, 3.45, 5.17 (250, 500, 750)

ports as in the 0.15-m (6-in.) single-port tests. This will provide information on scaling and the differences between single-port and multi-port testing. Multi-port injection configurations will be evaluated during this test series in addition to ignition system variables. A summary of the planned tests is presented in Table 3-8.

Additional goals for the 0.46-m (18-in.) multi-port test series include evaluation of throttling, fuel grain retention, and fuel crack propagation in a multi-port grain. Throttling will be achieved through facility control of the oxidizer flow rate. One or more grains will be fabricated with a grain retention system in place. Defects (cracks/voids) will be introduced into the grain to determine the effects on grain integrity and overall fuel utilization. Insulation, nozzle and consumable mandrel materials can also be evaluated during these tests.

Configuration and test parameters for this series are presented in Table 3-9. The grain will contain nine ports and the total grain length will remain the same, thus holding the port length-to-diameter ratio constant. The maximum oxidizer flow rate to provide proper mixture ratio and mass flux is 30.4 kg/s (67 lb/sec). This results in a maximum expected thrust from this

TABLE 3-8. PHASE 2 - TEST SERIES WITH 0.46-M (18-IN.) OD GRAINS (MULTI-PORT)

T17008

Test No.	G_{O2}, kg/s-m^2 (lb/sec-in.^{2})	$\dot{W}_{ign}$, kg/s (lb/sec)	Injector Configuration	Comment/Objective
1	X*	Y†	A†	Baseline/scale-up effects
2	X	‡	‡	Adjust igniter fuel flow and injector configuration
3	X	‡	‡	Optimize igniter fuel flow and injector configuration
4	Varied	Optimum	Optimum	Throttle test; insulation test§
5	X/2	Optimum	Optimum	Grain retention evaluation¶
6	X/4	Optimum	Optimum	Grain retention evaluation¶
7	Varied	Optimum	Optimum	Insulation test
8	Varied	Optimum	Optimum	Thrust profile, insulation test
9	Varied	Optimum	Optimum	Crack propagation/throttle test
10	TBD	TBD	TBD	TBD

* Value depends on fuel selected
† Start with optimum value from 6-in. test series
‡ Adjust as required for multi-port configuration
§ Material selection based on results of 6-in. test series
¶ Grains will be cast with and without retention system for evaluation

Instrumentation: P_4, F, P_{O2}, T_{O2}, injector plenum pressure (P_3), $\dot{r}$

motor of 125,434 N (28,200 lb). The fuel grain will contain 384 kg (845 lb) of fuel.

Instrumentation for this series will be identical to that described for the previous series. The tests will be conducted on CSD's RT-6 test stand.

TABLE 3-9. CONFIGURATION SUMMARY FOR 0.46-M (18-IN.) OD MULTI-PORT TESTS
T17026

Parameter	Value
Motor case diameter, m (in.)	0.46 (18)
Grain length, m (in.)	3.40 (134)
No. of ports	9
Total port area, m^2 ($in.^2$)	0.051 (79.2)
Port L/D_h	40
Maximum thrust, N (lb)	1.25×10^5 (28,200)
Maximum O_2 flow rate, kg/s (lb/sec)	30.4 (67)
Fuel weight, kg (lb)	383.6 (845)
Pressure, MPa (psia)	5.17 (750)*
*At maximum flow rate	

The next step in the scaling procedure will be to cast and test single-port 0.46-m (18-in.) OD grains. Comparison of this data to that obtained in 0.15-m (6-in.) hardware will allow scaling laws to be established and incorporated into the ongoing model development effort. In addition to ballistic scaling, scaling laws for igniter and injector components will be evaluated and, if necessary, empirical optimization of the associated configurations and operating conditions will be pursued. A summary of this test series is presented in Table 3-10.

Instrumentation for these tests will be identical to that specified for the previous tests and the test site will also remain the same. A summary of the test configuration is shown in Table 3-11. The single-port grain will have a port area of 1.75×10^{-2} m^2 (27.2 $in.^2$) and a grain length of 3.89 m (153 in.). A maximum of 8.9 kg/s (19.5 lb/sec) of oxidizer will be required to provide the correct flux and mixture ratio in the port, and this will result in a maximum thrust level of 36,474 N (8200 lb).

The final test series to be conducted in Phase 2 will be performed with 1.22-m (48-in.) OD multi-port grains having the same port size and configuration as the single port 0.46-m (18-in.) grains. Further evaluation of scale-up laws will be possible through comparison of this data with the 0.46-m

TABLE 3-10. PHASE 2 - TEST SERIES WITH 0.46-M (18-IN.) OD GRAINS (SINGLE-PORT)

T17009

Test No.	G_{O2}, kg/s-m^2 (lb/sec-in.^{2})	$\dot{W}_{ign}$, kg/s (lb/sec)	Comment/Objective
1	X*	Z†	Evaluate scale-up of igniter fuel flow rate
2	X	B‡	Optimize igniter fuel flow rate/oxidizer ramp rate
3	X/2	Optimum	GO_2 effects
4	X/4	Optimum	Fuel utilization
5	Varied	Optimum	Throttle/fuel utilization
6	Varied	Optimum	Repeatability
7	Varied	Optimum	TBD
8	Varied	Optimum	TBD

* Value depends on fuel selected
† Scale up optimum value from 6-in. tests
‡ Adjust as required

Instrumentation: P_4, P_3, P_{O2}, T_{O2}, F, $\dot{r}$

(18-in.) multi-port results. In addition to scaling effects, igniter optimization, throttling, fuel utilization and structural integrity of the grain will be evaluated. The planned test matrix is shown in Table 3-12. A summary of the test configuration is presented in Table 3-13. The grain will be a multi-port version of those tested in the previous 0.46-m (18-in.) OD combustor tests. Consequently the grain length will remain at 3.89 m (153 in.) and will have 10 ports with a total of 0.175 m^2 (272 in.^{2}). The maximum oxygen flow rate will be 88.5 kg/s (195 lb/sec), yielding a maximum thrust of 378,080 N (85,000 lb).

TABLE 3-11. CONFIGURATION SUMMARY FOR 0.46-M (18-IN.) OD SINGLE-PORT TESTS

T17032

Parameter	Value
Motor case diameter, m (in.)	0.46 (18)
Grain length, m (in.)	3.89 (153)
No. of ports	1
Total port area, m^2 ($in.^2$)	0.018 (27.2)
Port L/D_h	40
Maximum thrust, N (lb)	36,474 (8200)
Maximum O_2 flow rate, kg/s (lb/sec)	8.85 (19.5)
Fuel weight, kg (lb)	568.4 (1252)
Pressure, MPa (psia)	5.17 (750)*

*At maximum flow rate

Instrumentation required for the 1.22-m (48-in.) OD test series includes combustor pressure (P_4), head-end dome pressure (P_3), oxygen supply pressure (P_{O2}), oxygen supply temperature (T_{O2}), oxidizer flow rate, and fuel grain regression rate (ultrasonic).

Potential test sites for this series include the 2A stand at AFAL - Edwards Air Force Base and contractor test facilities such as Pratt & Whitney or CSD, as outlined in Table 3-14. The current recommendation is to perform these tests at AFAL on the 2A stand. This facility will be operational at the time planned for testing and will have cryogenic supply tanks of sufficient volume (over 18.9 m^3) to meet the requirements of the test motor. The size of the stand is also compatible with the specified motor size. Two disadvantages are that the stand is horizontal and there is no thrust measurement capability. If these measurements are determined to be essential or highly desirable for this test, the P&W stand would be the alternate. The CSD stand for this size of test requires significant modification and refurbishment and therefore would only be considered if existing facilities are not available.

TABLE 3-12. PHASE 2 - TEST SERIES WITH 1.22-M (48-IN.) OD GRAINS (MULTI-PORT)

T17010

Test No.	G_{O2}, kg/s-m^2 (lb/sec-in.^{2})	$\dot{W}_{ign}$, kg/s (lb/sec)	Comment/Objective
1	X*	C†	Baseline/evaluate scale-up effects
2	X	D‡	Optimize igniter fuel flow rate/oxidizer ramp rate
3	Varied	Optimum	Throttle test
4	Varied	Optimum	Fuel utilization/structural integrity
5	Varied	Optimum	Throttle fuel utilization
6	Varied	Optimum	Repeatability
7	Varied	Optimum	TBD
8	Varied	Optimum	TBD

* Value depends on fuel selected
† Scale up optimum value from 18-in. tests
‡ Adjust as required

Instrumentation: P_4, P_3, P_{O2}, T_{O2}, F, $\dot{r}$

3.4 OXIDIZER INJECTION TECHNOLOGY

3.4.1 Liquid Injectors

Prediction of the droplet size distribution (i.e., Sauter mean diameter (SMD) and range of droplet sizes) as a function of injector size, liquid and gas flow rates, and liquid properties is essential in rational design of a LOX injector. A pressure-swirl injector with gas assist is discussed in Appendix C since it is expected to produce smaller droplet sizes than an alternative like-on-like impinging injector. It also can more effectively use the waste heat in pumping system turbine exhaust gas to assist the atomization and vaporization processes.

TABLE 3-13. CONFIGURATION SUMMARY FOR 1.22-M (48-IN.) OD MULTI-PORT TESTS

T17031

Parameter	Value
Motor case diameter, m (in.)	1.22 (48)
Grain length, m (in.)	3.89 (153)
No. of ports	10
Total port area, m^2 ($in.^2$)	0.18 (272)
Port L/D_h	40
Maximum thrust, N (lb)	378,080 (85,000)
Maximum O_2 flow rate, kg/s (lb/sec)	88.5 (195)
Fuel weight, kg (lb)	3691 (8130)
Pressure, MPa (psia)	5.17 (750)*
*At maximum flow rate	

A database currently exists for pressure-swirl injectors with gas assist. However, data are not available for the injector sizes and liquid/gas flow rates indicated in Tables 3-15 and 3-16 for the various preliminary hybrid rocket designs. Hautman[10] has attempted to use state-of-the-art, laser-based droplet sizing instrumentation to study large rocket injectors, but with only limited success, as a consequence of the high spray densities characteristic of these devices. However, it is believed that high-quality data pertinent to large-injector-element performance can be obtained through experimental element modeling techniques that will permit acquisition of data in operating ranges more compatible with the capabilities of the laser-based droplet sizing equipment. Specifically, data from smaller scale elements would be obtained, as described below, and integrated with the database generated by Hautman[10] to form the basis for design correlations among SMD, spray droplet size distribution, injector size, and operating conditions. These correlations would be developed for ranges of injector size and operational conditions of such breadth that they could be confidently applied in the design of systems of the scale anticipated for a hybrid booster, even though that scale is likely to fall outside the range of the correlation database.

TABLE 3-14. POTENTIAL 1.22-M (48-IN.) DIAMETER BOOSTER TEST STANDS

T17036

Item	Facility/Location		
	Chemical Systems/ San Jose, CA	AFAL/ Edwards Air Force Base, CA	Pratt & Whitney/ West Palm Beach, FL
Stand	RT-6	2A	E8
Orientation	Vertical	Horizontal	Horizontal
Thrust compatibility	Modification required	No thrust measurement	1.11×10^6 N (250,000 lb) load
LOX supply	Tank required	23 m^3 (6000 gal)	3.4 m^3, 5.86 MPa (900 gal, 8500 psi); 18.9m^3, 3.4 MPa (5000 gal, 500 psi); 9.1 m^3 for H_2, 62.1 MPa (2400 gal, 9000 psi)
LOX delivery	Pressure	Pressure	Pressure
Availability	Available; refurbishment required	Available	Available
Other	Stand requires upgrade	-	Need pump for LOX pressure tank or use H_2 tanks

The United Technologies Research Center (UTRC) High Pressure Spray Facility would be used for these experiments. This facility, shown schematically in Figure 3-5, has been used for other rocket injector programs.[5,10] Either low-velocity (0.9-m/s (3-ft/sec) to 8-m/s (27-ft/sec)) nitrogen or air can be used as the bulk gas that flows through the facility. This bulk gas can be heated up to 811 K (1000°F) by an electric resistance heater. Sprays are generated in a test section that has windows on each side to provide optical access. The bulk gas removes the spray from the test section and helps keep the windows clear of liquid. The facility can operate from

TABLE 3-15. INJECTOR SIZED SO THAT 70% OF LIQUID IS VAPORIZED IN 1.02 M (40 IN.) AT A FLOW RATE OF 75% OF MAXIMUM FLOW RATE (LARGE BOOSTER)

T17047

Maximum flow, %	100	75	65
Mass flow/injector element, kg/s (lb/sec)	1.59 (3.5)	1.18 (2.6)	1.04 (2.3)
Predicted SMD, m (in.)	1.75 (69)	2.36 (93)	2.69 (106)
Maximum SMD for 100% vaporization, m (in.)	1.52 (60)	1.75 (69)	1.98 (78)
% vaporized	88	70	69

Note: injector diameter = 0.0107 m (0.42 in.)

TABLE 3-16. INJECTOR SIZED SO THAT 70% OF LIQUID IS VAPORIZED IN 0.51 M (20 IN.) AT A FLOW RATE OF 75% OF MAXIMUM FLOW RATE (SMALL BOOSTER)

T17048

Maximum flow, %	100	75	65
Mass flow/injector element, kg/s (lb/sec)	0.37 (0.82)	0.28 (0.62)	0.24 (0.53)
Predicted SMD, m (in.)	1.22 (48)	1.65 (65)	1.85 (73)
Maximum SMD for 100% vaporization, m (in.)	1.02 (40)	1.22 (48)	1.32 (52)
% vaporized	83	70	65

Note: injector diameter = 0.0051 m (0.2 in.)

atmospheric pressure to 3.4 MPa (500 psi), with the pressure being set by a back pressure regulator. A scrubber removes the liquid from the gas stream so that it can be collected and disposed.

Figure 3-6 presents photographs of the UTRC High Pressure Spray Facility with an Aerometrics phase doppler particle analyzer (PDPA) and a Malvern droplet size analyzer in place. The Aerometrics PDPA measures the droplet size and velocity distributions at a point in a spray. The Malvern droplet size analyzer measures line-of-sight droplet size distributions. The transmitter and receiver of the Aerometrics PDPA and the Malvern droplet size analyzer are mounted in such a way that both pieces can be moved simultaneously without affecting the optical alignment. This transmitter/receiver assembly is attached to a carriage that can move the assembly repeatably in the X, Y, and Z directions. Since line-of-sight droplet size distribution

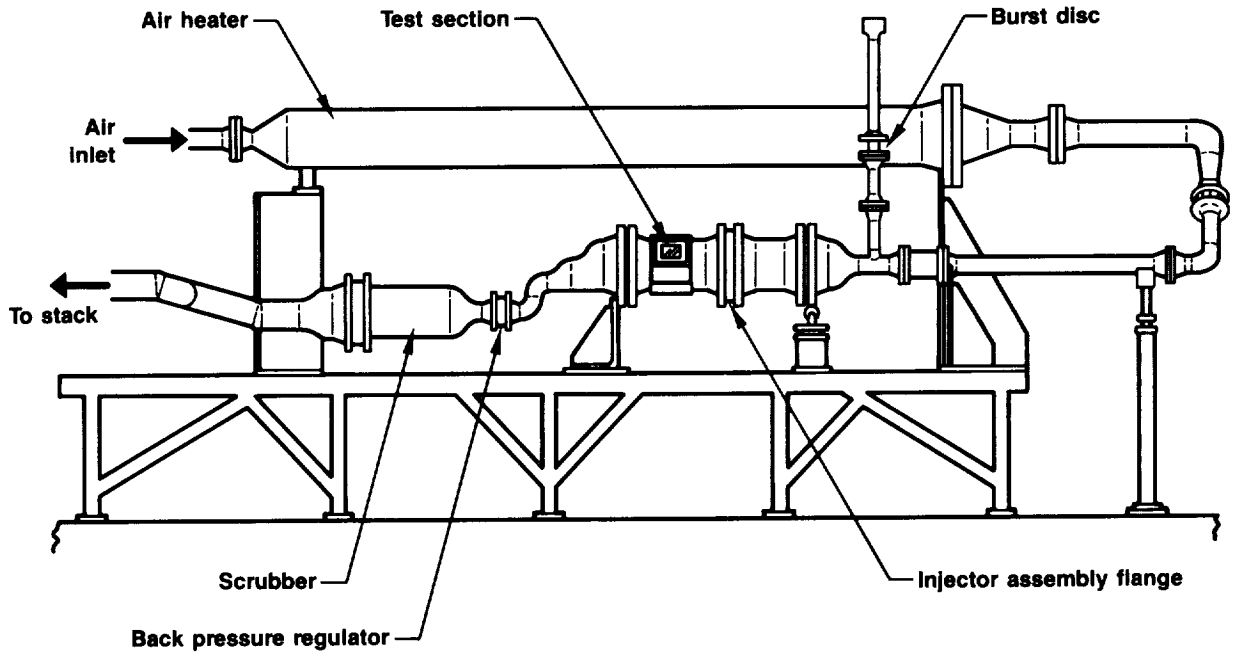

Figure 3-5. High-Pressure Spray Facility (Wide Range of Operating Conditions are Possible with this Facility)

50442

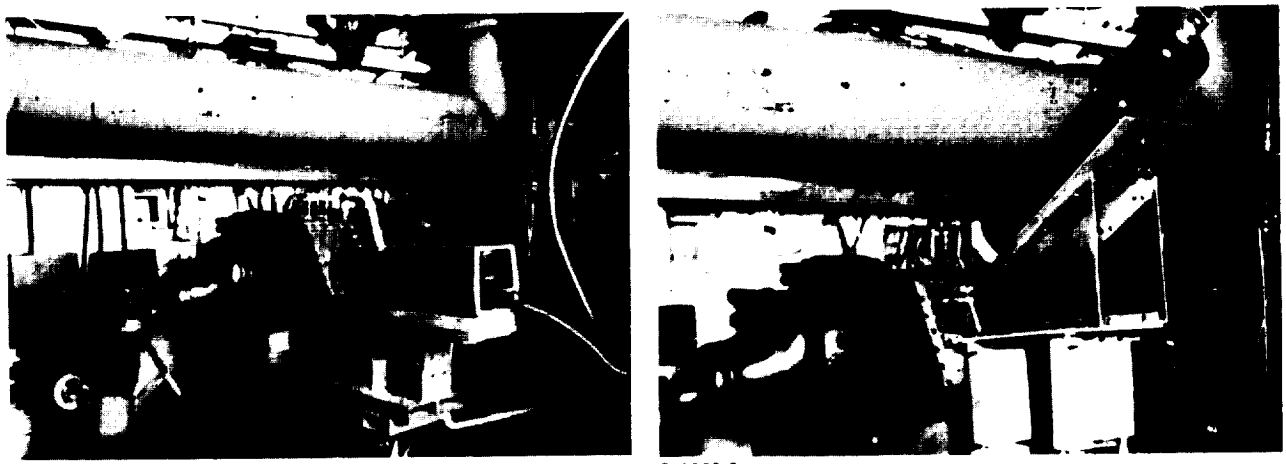

Figure 3-6. Droplet Sizing with Optical Diagnostics

50443

information is the required information, the Malvern droplet size analyzer would be the primary instrument used in the recommended program. However, a limited number of Aerometrics PDPA measurements would be made to confirm that the spray structure with small sized injectors is identical to that of large sized injectors. Since visual information can increase the confidence level

in laser-based diagnostics, photographs and videos would also be made of the generated sprays.

Sprays generated by gas-assisted pressure-swirl atomizers having orifice diameters an order of magnitude smaller than those tested by Hautman[10] would be characterized using a Malvern droplet size analyzer and an Aerometrics PDPA over a wide range of liquid/gas flow rates, chamber pressures/densities, and liquid properties. A schematic diagram of a candidate pressure-swirl injector with gas assist is given in Figure 3-7. The injector assembly consists of the following pieces:

- Liquid manifold
- Gas manifold
- Tube/bulkhead
- Injector support.

The swirl is generated by three tangential slots at the end of the tube. Figure 3-8 is a photograph of a disassembled injector. Geometric variations can be easily made by changing individual injector pieces. The injector is held by struts along the centerline of the high-pressure spray facility. Six such injector configurations would be investigated. These configurations would vary the injector size and the slot dimensions (i.e., the flow rate/ pressure drop ratio).

Various liquids and nitrogen gas would be supplied to the injector by independent delivery systems. Water, Jet A, and Freon 113 would be used as injectant simulants in this investigation in an attempt to obtain data over a wide range of liquid properties and operational conditions.

Proposed test matrices are given in Tables 3-17 and 3-18. Four levels of liquid flow rate, gas flow rate, and chamber density would be investigated for each liquid/injector combination. Aerometrics PDPA measurements would only be made with one liquid and injector configuration (i.e., Table 3-17). Malvern

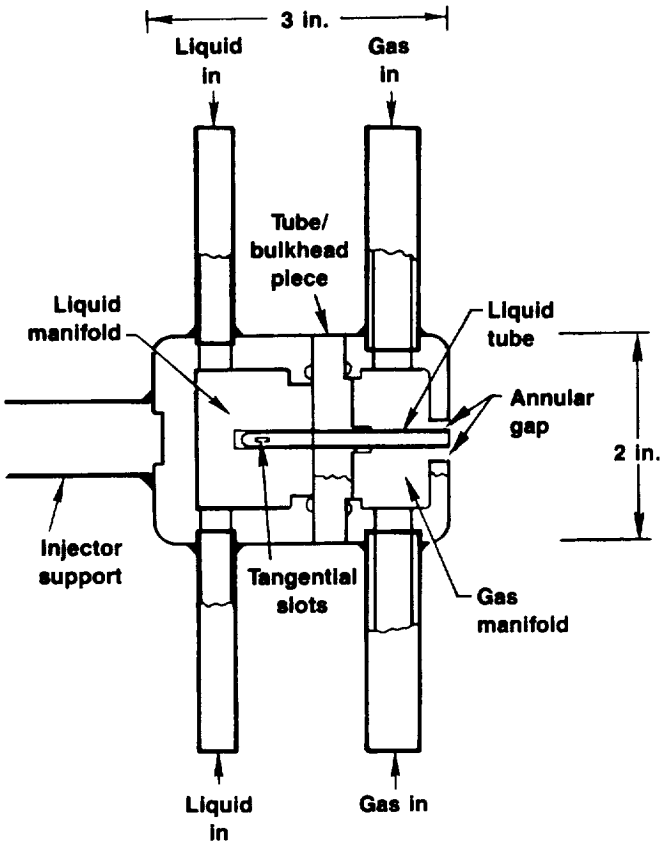

Figure 3-7. Injector Assembly Schematic

50444

droplet size analyzer measurements would be made with each liquid/ injector combination (i.e., Table 3-18).

3.4.2 Gaseous Injectors

Even though numerical codes exist that are believed capable of predicting the details of the flow field in the dome of a hybrid booster rocket employing multiple gas injection elements and having multiple grain ports, comparison of predictions with experimental data for such complex geometries has not been done to verify code efficacy. In addition, calculations with these codes have not been performed to determine what size and location of gaseous injectors would ensure uniform oxygen distribution to multiple-grain ports. Therefore, a two-step program is recommended to address these issues. First, code verification activities would be done to verify the chosen code efficacy. These activities would involve cold flow experiments using laser velocimetry and tracer gases to determine velocity, turbulence, and flow distribution. These tests would involve gaseous injection, through a multi-hole faceplate, toward a port(s) with a non-circular cross-section(s). The data from these tests would then be compared with the flow predictions of the numerical code to ensure the utility of the code for gaseous injector design. A proposed test matrix for the cold flow verification experiments is given in Table 3-19. Four levels of gas flow rate and pressure drop across the port would be investigated for each flow geometry. The second set of activities would involve the use of the numerical

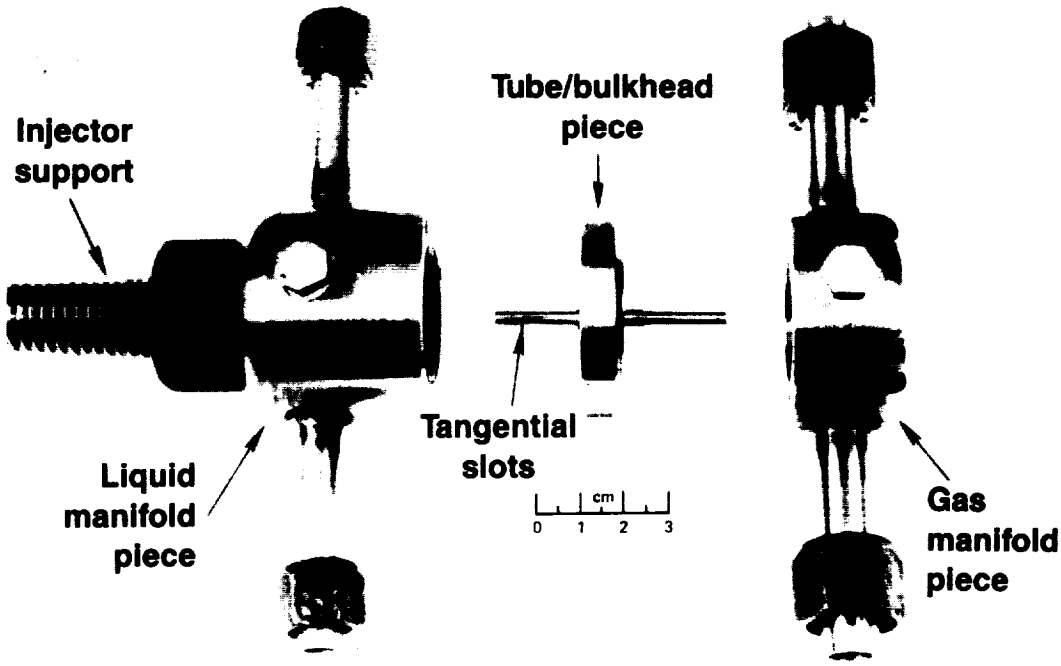

Figure 3-8. Injector Pieces can be Easily Exchanged for Geometric Variations
19282-3 50445

TABLE 3-17. TEST MATRIX FOR MALVERN DROPLET SIZE ANALYZER MEASUREMENTS TO BE DONE FOR EACH LIQUID/INJECTOR COMBINATION

T17033

Liquid Flow Rate				Gas Flow Rate				Chamber Density			
1	2	3	4	1	2	3	4	1	2	3	4
X				X				X	X	X	X
X					X	X	X	X			
	X	X	X	X				X			

TABLE 3-18. TEST MATRIX FOR AEROMETRIC PHASE DOPPLER PARTICLE ANALYZER MEASUREMENTS TO BE DONE FOR ONE LIQUID/INJECTOR COMBINATION

T17034

Liquid Flow Rate				Gas Flow Rate				Chamber Density			
1	2	3	4	1	2	3	4	1	2	3	4
X				X				X	X	X	X
X					X	X	X	X			
	X	X	X	X				X			

TABLE 3-19. TEST MATRIX FOR FLOW VISUALIZATION MEASUREMENTS TO BE DONE WITH EACH FLOW GEOMETRY

T17035

Gas Flow Rate				Pressure Drop Across Port			
1	2	3	4	1	2	3	4
X	X	X	X	X			
X					X	X	X

code to simulate the actual dome design. These calculations would determine the optimum size and location of the gaseous injectors needed to ensure uniform oxygen distribution to multiple grain ports.

3.5 IGNITION

The primary development issues for the recommended approach is the required number of pyrogen igniters, optimum igniter fuel flow rate, and sequencing and ramping of the oxidizer flow rate with the fuel flow rate and the pyrogen igniters.

The first test series designed to answer some of these questions will be conducted with a small-scale test apparatus and transparent fuel grains. A transparent hydrocarbon fuel grain is easily obtained in the form of Plexiglas tubes. This will be coupled to a forward dome fitted with oxidizer injectors and a representative ignition system. Flow rates of the igniter fuel and ramp rates of the oxygen will be varied and the effect on grain ignition will be observed. The transparent tube will permit visualization of flame spread during the moments following ignitor firing. A qualitative assessment of igniter effectiveness will be made for each operating condition and the full

results will be used to determine the optimum flow rate ratios and sequencing. Each test will be recorded on video and by high-speed movie for later assessment of the igniter effectiveness. The optimum igniter parameters will be used as the starting point for the 0.15-m (6-in.) single-port combustion tests.

During each of the combustion tests series described previously, igniter effectiveness will be assessed from the outset to assure that maximum performance is being obtained. The effectiveness will be evaluated based on pressure rise within the combustor at the start of each test. If these results indicate poor or incomplete ignition of the grain, appropriate modifications will be made to arrive at the optimum conditions. Modifications will include igniter fuel flow rate, oxygen flow ramp rate, pyrogen sequencing, and, if necessary, igniter location.

3.6 INSULATION

Four insulation materials have been identified as candidates for the hybrid booster. These include trowelable Kevlar-filled EPDM, standard Kevlar-filled EPDM, silica-filled EPDM, and carbon fiber-filled HTPB insulation (low regression rate). Each of these materials will be evaluated in the initial combustion test series followed by selection of one or more materials for use and additional evaluation during the series to follow. Trowelable EPDM has been identified for use in the head-end region only and therefore will be evaluated in that location alone. The other insulation materials will be evaluated by locating them downstream of the fuel grain so that the erosion/regression rates can be measured under hybrid motor operating conditions. Table 3-6, shown previously, indicates the tests in which these materials would be evaluated. If additional combustion testing is required, cartridges will be prepared for subsequent test series and consequently tested at a larger scale. In addition to combustion testing, physical and thermal property testing will be conducted with each material and cure studies will be performed.

3.7 CONSUMABLE MANDRELS

One of the design options discussed in Volume I is the use of consumable mandrels for grain fabrication. These mandrels would remain in place after casting and would burn out quickly after ignition. Use of consumable mandrels would simplify the grain casting procedure, provide support of the grain during transport, and eliminate or sharply reduce the need for tapered ports.

Candidate materials for these mandrels would be based on an epoxy resin binder filled with a fiber such as polyethylene or other hydrocarbon polymers. The final formulation would be determined based on a combination of burn rate results and mechanical properties. Mechanical properties will dictate the minimum thickness required for structural integrity during casting and the ballistic analysis will determine the burn rate required to meet mission goals.

The candidate mandrel materials will be tested starting with the 0.15-m (6-in.) OD combustor tests described previously. The grains to be used for these tests will be cast with and without consumable mandrels. The start and stop capability of the hybrid will allow the motor to be shut down soon after ignition so that the grain can be inspected and the burnout pattern observed. Pressure and thrust data will also indicate time for mandrel consumption, assuming that the burn rates of the fuel and the mandrels are not identical. Furthermore, ultrasonic regression rate data will provide precise burning rate data of the mandrel materials.

If this concept proves to be a desirable one for the hybrid booster, further testing will be pursued in the subsequent scale-up test series. This will also allow processing with larger scale consumable mandrels to be evaluated.

3.8 NOZZLE MATERIALS

Several materials have been recommended for use in the hybrid rocket motor nozzle depending upon location within the nozzle and whether or not LOX

TVC is selected for the final design. All of these materials will be evaluated during the four series (0.15-m (6-in.) OD through 1.22-m (48-in.) OD) of combustion tests described previously.

Regardless of the type of TVC selected, graphite-phenolic tape has been recommended for use in the throat and entrance sections of the nozzle. Consequently the first subscale nozzles fabricated will have graphite-phenolic entrance and throat sections for early evaluation of this material. Backside components of the submerged portion of the nozzle have been recommended to be made of PAN carbon-phenolic tape. The subscale nozzles will therefore include this design detail for early evaluation. The recommended exit cone material is either low-density PAN carbon-phenolic or silica-phenolic depending on the type of TVC selected for the final design. Both materials will be evaluated during the combustion tests and the results will be used to guide the material and possibly the TVC selection. The effect of LOX injection in the diverging section of the nozzle will be investigated during several of the early combustion tests with nozzles having silica-phenolic exit cones. A simple LOX injection line with a control valve will be used to make this evaluation. The motor will be instrumented with side-mounted load cells during these tests in order to evaluate the effectiveness of LITVC as well.

Nozzle support shells will be made from D6aC steel or equivalent. Each nozzle will be instrumented with backside thermocouples in the external regions of the exit cone. Primary regions of the nozzle will be dimensionally measured before and after each test to establish erosion rates, and this will be correlated with the specific motor operating conditions.

3.9 SYSTEMS CONTROL TECHNOLOGY

The development of specific control logic for hybrid boosters depends on detailed information on dynamic models of the system components, controlled system performance and reliability requirements, and specifications of sensor and actuator properties. Much of the design experience from liquid and solid rocket motors can be applied in the development of a control system for the

hybrid rocket motor. However, a number of unique features and capabilities of hybrid rocket motors must be examined further to clarify control system design issues.

A more precise model of the hybrid rocket motor thrust chamber dynamics must be constructed to assess the complexity of the thrust magnitude control logic. The input to this system element is the oxidizer flow rate (Wo). The controlled output is the chamber pressure (Pc). A unique feature of the hybrid motor is that the dynamics of this key element in the hybrid motor vary with time. Control of this non-stationary process will be dependent on the degree of variation in steady-state gain (dPc/dWo) and transport time constant over the entire burn time. Characterization of these dynamics will drive the design of control logic for both nominal and off-nominal operation (in the presence of failed system components).

It is recommended that a dynamic model of the thrust chamber be developed that couples advanced regression rate models with grain port control volume and gas path dynamics. Where appropriate, data from solid booster motor firings will be utilized for validation. The projected program for hybrid motor thrust chamber dynamic modeling could be completed within 5 months using approximately four man-months of engineering effort.

The second major technology issue that should be addressed in preparation for hybrid booster development is vehicle TVC requirements. Unlike vehicles powered by solid rocket boosters, hybrid-powered vehicles will have feedback control of the effective thrust on each booster. Thus it is anticipated that a reduced level of TVC will be required to account for motor thrust imbalances. Further, vehicles with hybrid rocket boosters would have the capability for altering the effective thrust vector by modulating the motor-to-motor thrust magnitude in cluster arrangements. This added design flexibility might be utilized to reduce the burden on the nozzle LOX injection flow rates if a LOX injection TVC system were used.

An analysis of TVC requirements for a vehicle with hybrid boosters is recommended. The first step would be creation of a vehicle model and configuration. Next, data would be acquired that are representative of the disturbances that would be typical of envisioned vehicle missions. Various thrust magnitude and vector control options would then be analyzed to determine specifications for the TVC system.

3.10 PHASE 3 RECOMMENDATIONS

Following the completion of testing in Phase 2, an assessment of existing test hardware and test sites will be made concerning their applicability to a large subscale hybrid motor demonstration. A preliminary selection of hardware and test site along with associated cost and schedule estimates will be made as a recommendation for further work in Phase 3.

3.11 SCHEDULE AND COST

The preliminary schedule for the Phase 2 program has been prepared and is presented in Figure 3-9. Each identified technology area is shown along with a breakdown as to the specific work required, and the relative time each of these subtasks would be conducted. The Phase 2 program would be a 3-year effort encompassing all of the tests and analyses described above. The major component development efforts are listed separately but, for the most part, will be performed as integrated parts of the combustor testing.

An associated cost of the development effort described in this report has been estimated based on the expected number of hours required for each subtask and the type and amount of material and hardware needed to support each of the test series. A summary of this cost estimate is presented in Table 3-20. An estimate of labor and non-labor costs for each identified technology is listed in this table. The estimate indicates that development of the grain ballistics technology comprises over half of the total effort in terms of funds required. This is true because the bulk of the test hardware

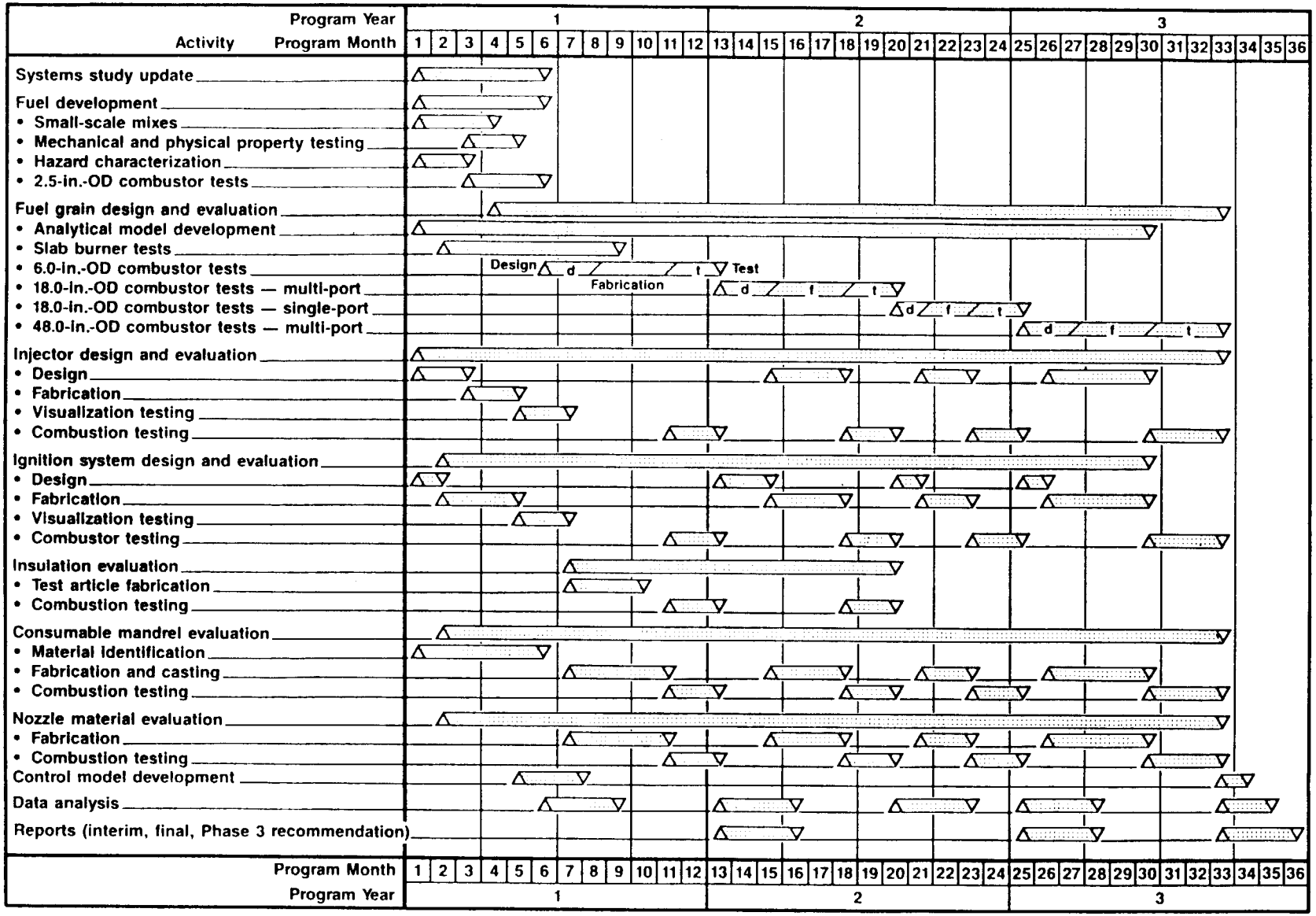

Figure 3-9. Phase 2 Schedule

50458

TABLE 3-20. PHASE 2 COST SUMMARY

T17087

Item	Labor, K$	Nonlabor, K$
System study update	167.4	55.2
Fuel development	358.4	58.0
Grain design and ballistics	1217.5	1638.0
Injector development	321.6	379.0
Ignition development	56.0	98.0
Insulation	142.8	25.0
Consumable mandrels	94.8	93.0
Nozzle development	70.4	945.0
Control systems	47.6	10.2
Reports	148.9	12.0
Program management	117.0	-
ODC	-	85.0
Totals	2742.4	3398.4
Grand total	6140.8	

will be designed, fabricated, assembled, and tested under this task. The cost for the development of the other major components includes only those costs specific to those tasks.

4.0 LARGE SUBSCALE MOTOR DEMONSTRATION PLAN

The primary objective of the Phase 3 program is to demonstrate a large subscale motor that best meets the design evaluation requirements of the two different booster sizes and that best incorporates the critical features of either or both designs. A flow diagram outlining the Phase 3 effort is presented in Figure 4-1. The program will essentially be a sequential series of tasks starting with definition of the test hardware and site and concluding with the demonstration tests.

Figure 4-1. Phase 3 Large Subscale Motor Demonstration Flowchart

50455

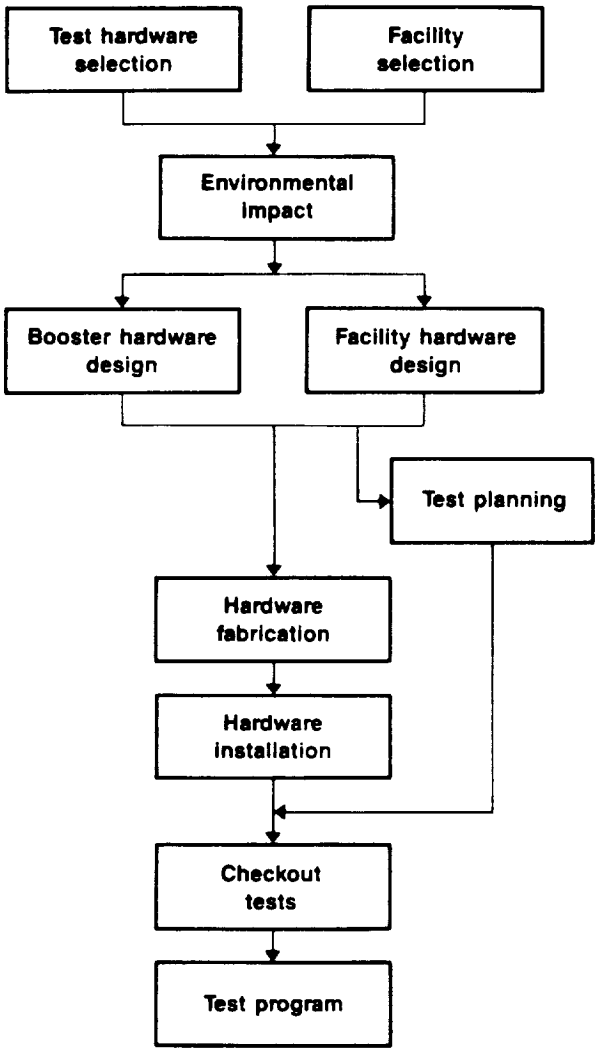

4.1 TEST HARDWARE DEFINITION

The first step in planning for the large subscale motor demonstration is the assessment and selection of available test hardware. Existing hardware will be used so as to minimize the cost of this effort. Three sizes of existing hardware have been identified as candidates for the large subscale demonstration as indicated in Table 4-1. A 1.22-m (48-in.) diameter (nozzleless booster), a 2.06-m (81-in.) diameter (Super HIPPO), or a 3.05-m (120-in.) diameter (Titan) motor could be used.

Multi-port grains in 1.22-m (48-in.) hardware are not recommended in this phase because it would be

TABLE 4-1. SUBSCALE HYBRID MOTOR TEST OPTIONS FOR PHASE 3

T16189

Motor Diameter/ Grain Configuration	Scale Approximate	Regression Profile	Fuel Utilization	Ballistic Performance	Nozzle Performance	Ignition System Assessment	Insulation Performance Assessment	Relative Cost*
1.22m (48 in.)/ single port	Full - 2S†, 1.4 - 8S†	Yes	No	Partial	Partial	Single port	Partial	3
2.06m (81 in.)/ multi-port grain grain	0.5 - 2S, 0.73 - 8S	Yes	Yes	Yes	Yes	Yes	Yes	5
3.05m (120-in.)/ multi-port grain, 10 port setments, circular center port	0.8 - 2S, full - 8S	Yes	Yes	Yes	Yes	Yes	Yes	8

* Based on 10 = full-scale costs
† Two-booster motor assembly or eight-booster motor assembly

little more than duplication of the Phase 2 efforts. Single-port 1.22-m (48-in.) grains are an option, but this option is also not recommended because the effects of multi-port grains on ignition, injection, fuel utilization, grain structural integrity, and combustion efficiency cannot be demonstrated.

At this time, the 2.06-m (81-in.) diameter hardware has been eliminated because, first, the condition of this hardware is unknown and, second, this hardware is less than half-scale of the large size booster and is considered by CSD to be too small to adequately demonstrate that the hybrid technology can be successfully scaled up to booster sizes.

The recommended size for the large subscale motor demonstration is 3.05-m (120-in.) diameter, thus allowing Titan case segments to be used. Not only is the hardware available, but the processing, handling, and transportation of these segments is ongoing and therefore the associated cost for these activities are expected to be lower as well.

A conceptual sketch of how four Titan case segments, a Titan aft closure and nozzle, and a specially fabricated head-end would be fitted together is presented in Figure 4-2. Each segment would be cast individually and the ports would be lined up on assembly. An adapter ring would be fabricated and placed between the Titan aft closure and nozzle to eliminate the cant angle present in the Titan design. Oxygen would be delivered to the motor from a high-pressure tank either by simply valving a line from the tank to the injector or by including a heat exchanger or heavyweight GOX pump upstream of the injectors to provide them with GOX. The selection will be based on the selections made in Phase 2 as to the type of oxygen feed system.

A preliminary set of test conditions has been determined for a 3.05-m (120-in.) demonstrator motor. These conditions are summarized in Table 4-2. A full-duration test firing of 120 sec will require 136,200 kg (300,000 lb) of LOX (120 m^3 (31,700 gal)) and will result in a maximum of 6.05 million N (1.36 million lb) of thrust. Motor length, excluding the forward dome and injector

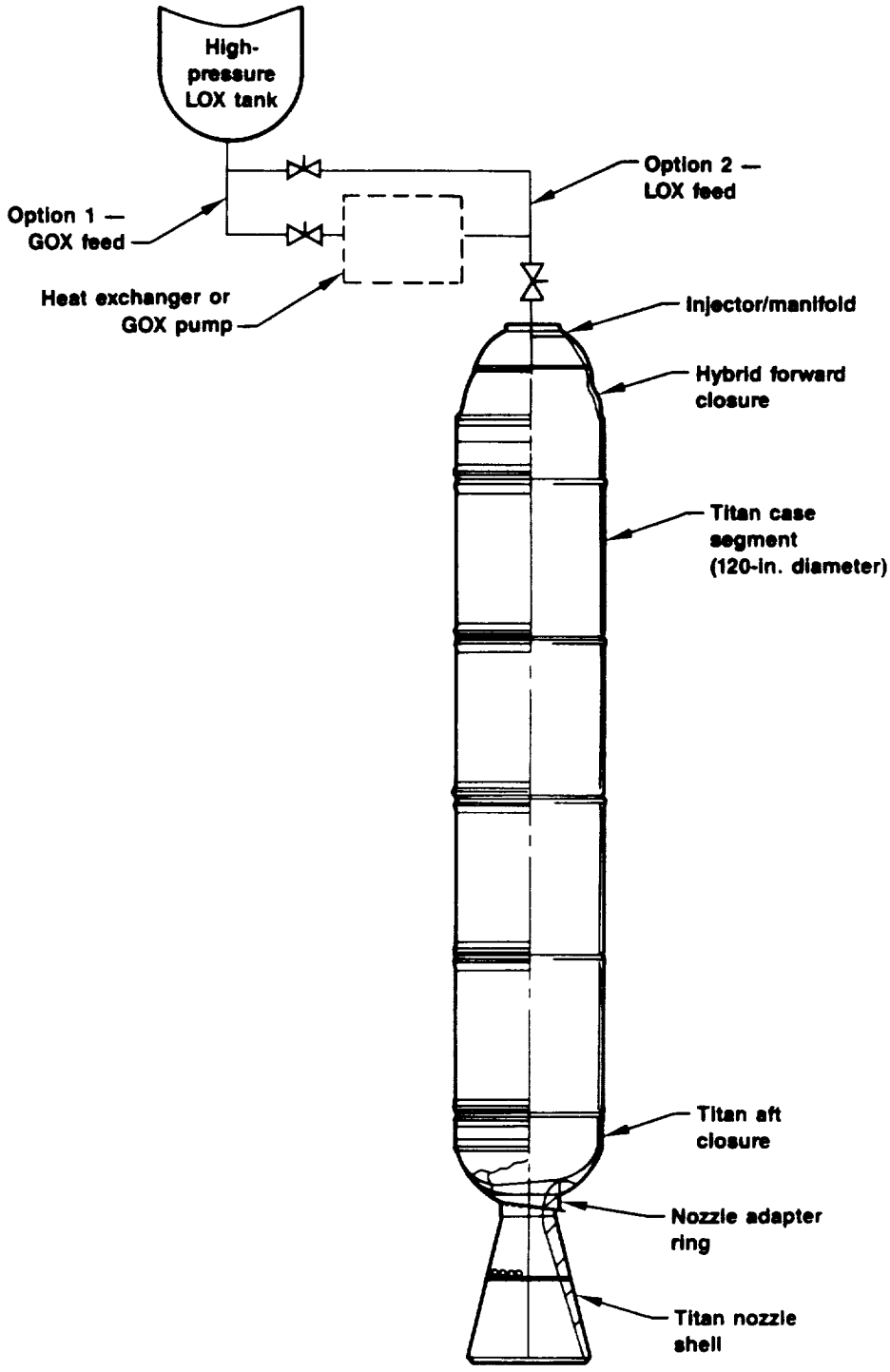

Figure 4-2. Phase 3 Motor Demonstration Concept Flowchart

50456

TABLE 4-2. PRELIMINARY TEST CONFIGURATION FOR PHASE 3

T17011

Parameter	Value
Motor case diameter, m (in.)	3.05 (120) (Titan)
Number of segments	4 plus aft closure
Segment weight (loaded), kg (lb)*	17,895 (39,416)
Aft closure weight (loaded), kg (lb)	5435 (11,972)
Length of segments plus aft closure, m (in.)	14.5 (570)
Nozzle length, m (in.)	3.2 (125.8)
Average thrust, N (lb)	4.24×10^6 (0.954×10^6)
Maximum thrust, N (lb)	6.05×10^6 (1.360×10^6)
Maximum O_2 flow rate, kg/s (lb/sec)	1453 (3200)
Average O_2 flow rate, kg/s (lb/sec)	1003 (2209)
Total LOX weight required for full-duration test, kg (lb)	1.36×10^5 (3.0×10^5)
Total LOX volume required, m^3 (gal)	120 (31,700)
Total fuel weight, kg (lb)	62,590 (137,863)

* Assumes fuel No. 7 is used

section, would be 17.7 m (695 in.). An additional 1.5 to 2 m (60 to 80 in.) would be required for the forward section.

Another alternative to the 3.05-m (120-in.) Titan hardware potentially will exist at the time these tests are expected to be conducted, namely, the use of an ALS case and associated hardware. This may be an especially attractive choice if the quad engine configuration for the large booster (2.44-m (96-in.) diameter) is selected as a result of the mission study update

conducted in Phase 2. This alternative will be assessed during the hardware selection portion of the Phase 3 program.

4.2 TEST SITE DEFINITION

A survey of potential test sites for the demonstration test has been made which included AFAL at Edwards Air Force Base, the Booster Technology Simulator (BTS) stand to be built at the NASA Marshall Space Flight Center, and the NASA NSTL site (Stennis Space Center). A summary of this survey is presented in Table 4-3. The facilities at AFAL are generally large enough to

TABLE 4-3. POTENTIAL LARGE SUBSCALE BOOSTER TEST STANDS

T17037

Item	Facility/Location		
	NASA Marshall Space Flight Center/ Huntsville, AL	**Stennis Space Center/ Bay St. Louis, MS**	**AFAL/ Edwards Air Force Base, CA**
Stand	G2	B2 position	F1
Orientation	Vertical, nozzle down	Vertical, nozzle down	Vertical, nozzle down
Thrust compatibility	6.7×10^6 N (1.5×10^6 lb)	3.34×10^7 N (7.5×10^6 lb)	No thrust measurement
LOX supply	120 m^3 (32,000 gal)	Tank required	Tank required
LOX delivery	Pressure	Pressure	Pressure
Availability	1995	Available	Available; refurbishment required
Required modifications	None	Stand modifications and gas control systems	LOX tanks, delivery system
Other	-	-	Load cells are 15 years old

handle a firing of this size, but the stands lack cryogenic tankage of sufficient volume to handle a full-duration test. The NSTL site would likely be able to handle this size motor and supply the required volume of LOX; however, LOX feed tanks and pressurization system or turbopumps would have to be provided in addition to the hybrid motor. This would therefore be a more costly test than one conducted in a facility where feed tanks already exist. For these reasons the BTS facility at Marshall has been selected as the recommended test site for the large subscale motor demonstration. This facility has LOX tankage of sufficient volume to handle a full-duration test, the thrust stand is capable of holding a test motor with up to 6.7 million N (1.5 million lb) of thrust, and the size of the stand is compatible with the four-segment Titan configuration outlined above.

4.3 TEST PLAN

A preliminary test plan has been established for Phase 3. Two demonstration motors will be prepared and four tests will be conducted with these motors. A summary of the test conditions and test objectives is presented in Table 4-4. The first motor will be tested three times, at durations of 5, 40,

TABLE 4-4. PHASE 3 TEST MATRIX

T17030

Test No.	Motor No.	Burn Time, sec	GO_2, kg/s-m^2 (lb/sec-in.^{2})	Objective/Comment
1	1	5	562.5 (0.8)	Ignition, consumable mandrel demonstration, start/stop capability
2	1	40	562.5 to 281.2 (0.8 to 0.4)	Throttling, thrust profiling
3	1	75	281.2 to 140.6 (0.4 to 0.2)	End of burn grain integrity
4	2	120	562.5 to 140.6 (0.8 to 0.2)	Full-duration demonstration

and 75 sec, respectively. The first of these three tests will be performed to demonstrate the ignition system, the consumable mandrels, and the shutdown capability. The oxidizer flux rates will be held at 562.5 kg/s/m^2 (0.8 lb/sec-in.^{2}). The second test will demonstrate throttling capability and its effectiveness in providing thrust modulation. The oxidizer flux rate will be reduced to 281.2 kg/s/m^2 (0.4 lb/sec-in.^{2}) from an initial value of 562.5 kg/s/m^2 (0.8 lb/sec-in.^{2}). The third test with this grain will demonstrate grain integrity at end of burn conditions. If a structural reinforcement system has been determined to be necessary in Phase 2, such a system will be included and demonstrated in this test as well.

The final test of the demonstration will be performed with the second motor and will be a full-duration (120-sec) test. The oxidizer flux rate will be varied from 562.5 to 140.6 kg/s/m^2 (0.8 to 0.2 lb/sec-in.^{2}) in such a way as to provide a subscale matching of the required thrust profile.

In each of the four tests, all major components will necessarily be demonstrated in addition to the objectives listed in Table 4-4. This includes injectors, insulation, and nozzle. The Titan case segments and hybrid forward closure will be lined with insulation material selected on the basis of the test results in Phase 2. While the method of lining will depend on the material selected, it is expected that hand layup will be required. The insulated cases will have fuel grains cast into them at the CSD processing facilities and will be inspected and readied for shipping to the selected test site. A Titan nozzle shell will be used for the demonstration tests; however, the nozzle geometry insulation sections will be specially designed for the hybrid motor. Calculations indicate that with an initial expansion ratio of 12 for the 3.05-m (120-in.) diameter hybrid motor, the exit area would be nearly identical to that of Titan but the throat section would be smaller. Thicker nozzle insulation and throat sections will be designed and built to fit the Titan nozzle shell. The forward dome and oxidizer injection sections will be designed to mate with the Titan motor segment and will include an injector design selected based on the results of Phase 2. The ignition system will also match the selected booster design approach.

Two possibilities exist for the oxidizer feed system. If the results of Phase 2 indicate that LOX injection is the preferred method, then a simple pressure-fed arrangement will be used with available high-pressure facility LOX tanks. If GOX injection is determined to be necessary for combustion and ballistic reasons, then a heat exchanger will be built and inserted between the LOX tank and the motor for vaporization of the oxygen prior to injection. An alternative approach is to build a workhorse GOX pump system. At this time this is considered to be an optional approach.

Thrust measurement will be made during this test series and a sketch of the thrust take-outs and stand attachment arrangement is presented in Figure 4-3.

4.4 SCHEDULE AND COST

A preliminary program schedule for Phase 3 is presented in Figure 4-4. This effort would require 2 1/2 years to complete. By the end of the first year, booster and facility test hardware will be in fabrication and a test plan will have been written. This will be followed by installation of all hardware on the test stand, checkout tests, and finally the four demonstration tests.

Four Titan motor segments plus one aft closure will be refurbished and insulated with material specified as a result of Phase 2 testing. These segments will be tested in tests 1 through 3 and then will be sent back to CSD for refurbishment and recasting. The forward dome and nozzle sections will also be relined with the appropriate insulation prior to the final demonstration test.

A cost estimate has been prepared for each of the activities listed in the schedule (see Table 4-5). The total cost estimate is approximately $30 million and represents about an 86 man-year level of effort over the 2 1/2-year program. This estimate does not include the cost associated with NASA personnel during the motor demonstration program, but costs have been escalated.

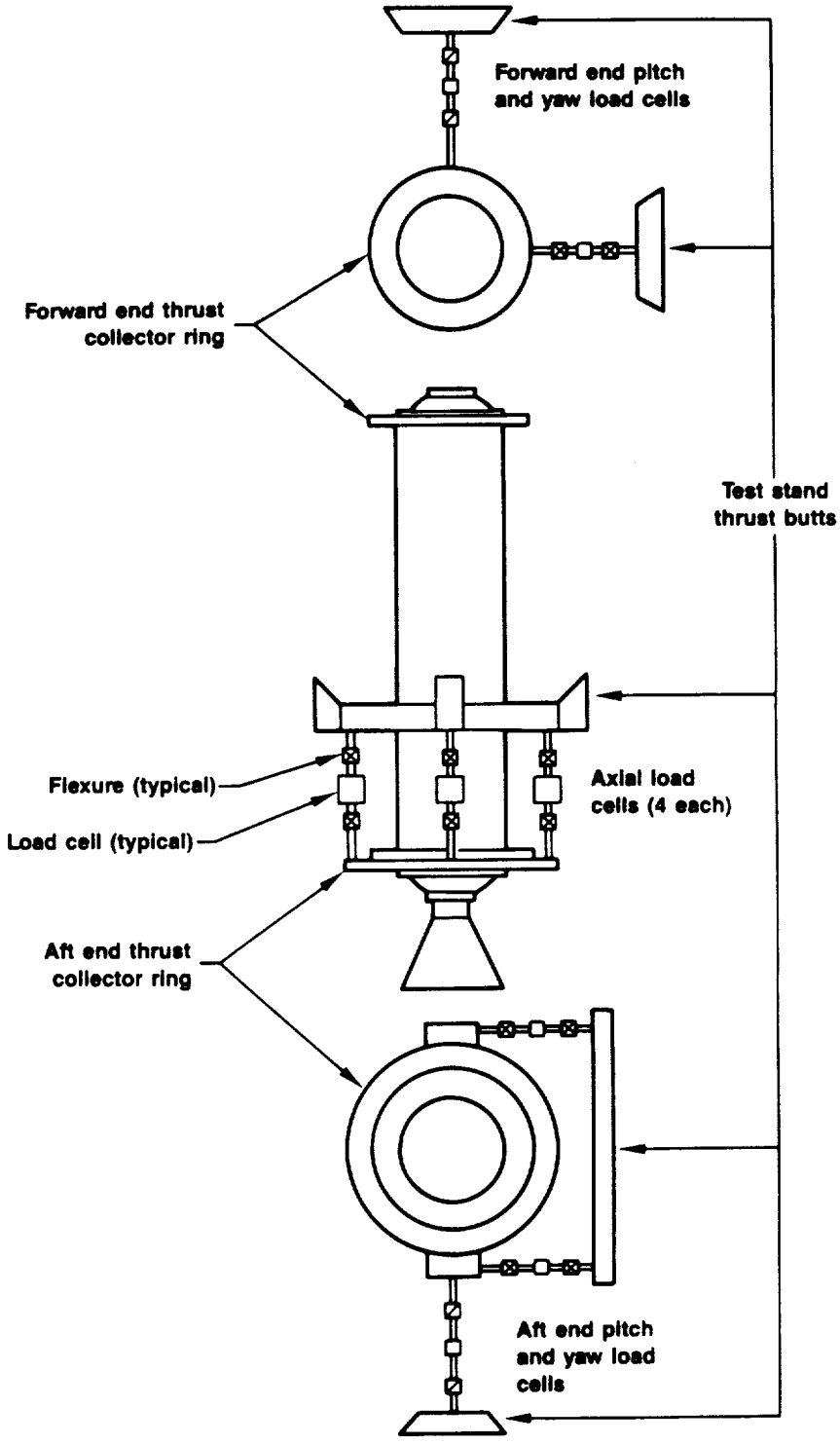

Figure 4-3. Thrust Measurement System Concept for Large Hybrid Rocket
50457

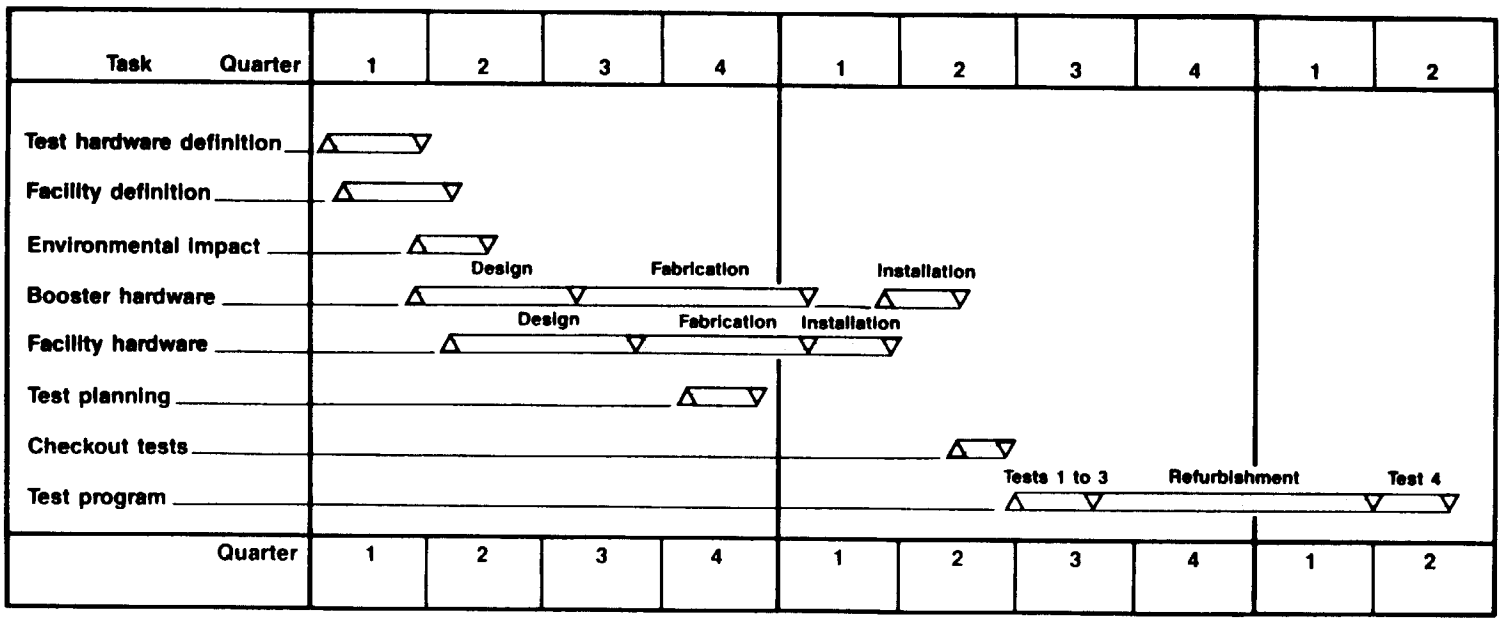

Figure 4-4. Test Program Overview for Subscale Motor Demonstration

46341

TABLE 4-5. PHASE 3 COST SUMMARY

T17088

Preliminary Engineering		$129,000
Environmental Impact Studies		$60,000
Booster Hardware		$21,169,000
Design and engineering support	3,072,000	
Refurbishment/insulation	7,440,000	
Nozzles	3,840,000	
Fuel grains	4,404,000	
Transportation	288,000	
Instrumentation/miscellaneous	1,000,000	
Assembly	1,255,000	
Test Costs		8,830,000
Facility modification/control hardware	5,100,000	
Assembly	1,255,000	
Test personnel - contract	927,000	
Oxygen/test materials	1,548,000	
Program Management/ODC		1,333,000
	Total	$31,621,000

Note: 1995 costs (total costs 1989 = $24,324,000)

REFERENCES

1. Ferrenberg, A., Hunt, K., and Duesberg, J., "Atomization and Mixing Study," Contract No. NAS8-34504, Dec. 1985.
2. Gill, G. S., and Nurick, W. H., "Liquid Rocket Engine Injectors," NASASP-8089, Mar. 1976.
3. Ingebo, R., and Foster, H., "Drop Size Distributions for Crosscurrent Breakup of Liquid Jets in Airstreams," NACA TN 4087, Oct. 1957.
4. Brault, F., and Lourme, D., "Experimental Characterization of the Spray Formed by Two Impinging Jets in a Liquid Rocket Injector," International Conference on Liquid Atomization and Spray Systems (ICLASS), London, July 8-10, 1985.
5. Hautman, D. J., "Spray Characterization of Impinging Rocket Injectors," 1989 JANNAF Propulsion Meeting, Cleveland, Ohio, May 1989.
6. Fraser, R. P., Dombrowski, A. H., and Routley, J. H., "The Atomization of a Liquid Sheet by an Impinging Air Stream," Chemical Engineering Science, 18, pp. 339-353, 1963.
7. Simmons, H. C., "The Prediction of Sauter Mean Diameter for Gas Turbine Fuel Nozzles of Different Types," ASME, 79-WA/GT-5, 1979.
8. Ingebo, R. D., "Atomization of Liquid Sheets in High Pressure Airflow," NASA Technical Memorandum 83731, 1984.
9. Lefebvre, A. H., "The Prediction of Sauter Mean Diameter for Simplex Pressure Swirl Atomizers," Atomization and Spray Technology, 3, pp. 37-51, 1987.
10. Hautman, D. J., "Spray Characterization of Liquid/Gas Coaxial Injectors with the Center Liquid Swirled," 25th JANNAF Combustion Meeting, Huntsville, Alabama, Oct. 1988.
11. Pantankar, S. V., Numerical Heat Transfer and Fluid Flow, New York, Hemisphere Publishing, 1980.
12. Amsden, A. A., O'Rourke, P. J., and Butler, T. D., "KIVA-II: A Computer Program for Chemically Reacting Flows With Sprays," Los Alamos National Laboratory Report LA-11560-MS, May 1989.
13. Peters, R. L., Design of Liquid, Solid and Hybrid Rockets, New York, Hayden Books, 1965

14. Zurawski, R. L., and Rapp, D. C., "Analysis of Quasi-Hybrid Solid Rocket Booster Concepts for Advanced Earth-to-Orbit Vehicles," NASA Technical Paper 2751.

15. Muzzy, R. J., "Applied Hybrid Combustion Theory," AIAA/SAE 8th Joint Propulsion Conference, Paper 72-1143, New Orleans, LA, Nov. 29 - Dec. 1, 1972.

16. Marxman, G. A., and Gilbert, M, "Turbulent Boundary Layer Combustion in the Hybrid Rocket," Western States Section, The Combustion Institute, 1962 Fall Meeting, Sacramento, CA.

17. Marxman, G. A., Wooldridge, C. E., and Capener, E. L., "Response of Burning Propellant Surface to Erosive Transients," Final Report, Stanford Research Institute, AFOSR Scientific Report No. 68-0771, April 30, 1968.

18. Wooldridge, C. E., and Marxman, G. A., "A Comparison Between Theoretical and Experimental Extinction Behavior of Composite Solid Propellants," AIAA 6th Propulsion Joint Specialists Conference, Paper 70-666, San Diego, CA June 15-19, 1970.

19. Schmucker, R. H., and Lips, H., "Hybrid Propulsive Systems Technology and Applications," Translation of European Space Agency Report DRL-IB-456-76/11, c. 1978.

20. Green, L., Jr., "Introductory Considerations on Hybrid Rocket Combustion," American Institute of Aeronautics and Astronautics Progress in Aeronautics and Astronautics, Vol. 15, Heterogeneous Combustion, New York, Academic Press, 1964, pp. 451-484.

21. Patankar, S. V., Numerical Heat Transfer and Fluid Flow, New York, Hemisphere Publishing, 1980.

22. Cherng, D. L., Yang, V., and Kuo, K. K., "Theoretical Studies of Turbulent Reacting Flows in a Solid-Propellant Ducted Rocket Combustor," AIAA/SAE/ASME/ASEE 23th Joint Propulsion Conference, Paper 87-1723, San Diego, CA, June 29-July 2, 1987.

23. Cherng, D. L., Yang, V., and Kuo, K. K., "Simulations of Three-Dimensional Turbulent Reacting Flows in Solid-Propellant Ducted Rocket Combustors," AIAA/ASME/SAE/ASEE 24th Joint Propulsion Conference, Paper 88-3042, Boston, MA, July 11-13, 1988.

24. Nabity, J. A., "Combustor Modeling of a Solid Fuel Ramjet Engine," Twenty-Third JANNAF Combustion Meeting, D. L. Decker, ed., Chemical Propulsion Information Agency, CPIA Publication 457, Oct. 1986.
25. Sabnis, J. S., Gibeling, H. J., and McDonald, H., "Navier-Stokes Analysis of Two and Three-Dimensional Flow Field in Solid Rocket Motors with Segment Joints," AIAA/SAE/ASME/ASEE 23th Joint Propulsion Conference, Paper 87-1804, San Diego, CA, June 29-July 2, 1987.
26. Amsden, A. A., O'Rourke, P. J., and Butler, T. D., "KIVA-II: A Computer Program for Chemically Reacting Flows With Sprays, Los Alamos National Laboratory, Report LA-11560¢MS.
27. Nickerson, G. R., Coats, D. E., Dang, A. L., Dunn, S. S., Berker, D. R., Hermsen, R. L., and Lamberty, J. T., "The Solid Propellant Rocket Motor Performance Prediction Computer Program (SPP) Version 6.0, Volume I," Engineering Manual, Air Force Astronautics Laboratory Report AFAL-TR-87-078, Dec. 1987.
28. Sturgess, S. J., Syed, S. A., and McManus, K. R., "Calculation of Hollow-Cone Liquid Spray in a Uniform Air Stream," AIAA/ASME/SAE 20th Joint Propulsion Conference, Paper 84-1322, Cincinnati, Ohio, June 11-13, 1984.
29. Razdan, M. K., and Kuo, K. K., "Turbulent Boundary-Layer Analysis and Experimental Investigation of Erosive Burning Problem of Composite Solid Propellants," Air Force Office of Scientific Research Report AFOSR-TR-79-1155, March 1979.
30. Razdan, M. K., and Kuo, K. K., "Turbulent-Flow Analysis and Measurements of Erosive Burning Rates of Composite Solid Propellants, AIAA/SAE/ASME 16th Joint Propulsion Conference, Paper 80-1209, Hartford, CT, June 30-July 2, 1980.
31. Razdan, M. K., and Kuo, K. K., "Chapter 10 - Erosive Burning of Solid Propellants," Progress in Aeronautics and Astronautics, Vol. 90, Fundamentals of Solid-Propellant Combustion, K. K. Kuo and M. Summerfield, eds., New York, American Institute of Aeronautics and Astronautics, 1984, pp. 515-598.
32. King, M. K., Kuo, K. K., and Beddini, R., "Experimental and Analytical Study of Erosive Burning of Solid Propellants," Final Report, October 1, 1978 - January 30, 1981, Air Force Office of Scientific Research AFOSR-TR-81-0609, June 1981.

33. Kuo, K. K., and Arora, R., "Turbulent Boundary-Layer Analysis and Experimental Investigation of Erosive Burning of Composite Solid Propellants, Final Report from Penn State to ARC under contract No. F49620-78-C-0016, April 1, 1981.

34. Patankar, S. V., and Spalding, D. B., Heat and Mass Transfer in Boundary Layers, London, Intertext Books, 1970.

35. Godon, J. C., Duterque, J., and Lengelle, G., "Solid Propellant Erosive Burning, AIAA/SAE/ASME/ASEE 23th Joint Propulsion Conference, Paper 87-2031, San Diego, CA, June 29-July 2, 1987.

Appendix A

HYBRID GRAIN REGRESSION ANALYSIS : A LITERATURE REVIEW

The flow within a hybrid rocket motor fuel grain is the result of the complex interaction of several physical processes. These processes include heat and mass transfer between the gas and solid surface and between the gas and liquid or particulate phases. Heat transfer by both convection and radiation is important. Near the head-end of the combustor, the droplet number density may be large enough that the effects of droplet-droplet and droplet-surface interactions are significant. Secondary flows within complex ports may also be important. Therefore, a general model of the hybrid grain regression process would be a sophisticated, three-dimensional, two-phase flow analysis for turbulent, reacting, recirculating flow coupled directly to a model describing important processes within the grain. The coupling can be accomplished by source terms in the governing equations and appropriate boundary conditions. However, many motor designs of interest lend themselves to more simplified analysis. Therefore, a literature review was performed to identify both one-dimensional and multi-dimensional analyses that have been, or can be, applied to the modeling of rocket motors.

A.1 ONE-DIMENSIONAL ANALYSES

Relatively few analyses appear in the more recent literature. Generally, the results of earlier studies can be classified as either cycle analyses (e.g., references 13 and 14), which may include correlations of burning rate data and zero- or one-dimensional analyses based upon the assumption that the regression rate is determined primarily by the rate of heat transfer between the port flow (i.e., the flow in the axial direction) and the solid fuel.[15-18,19] The model due to Muzzy[15] is referred to as a boundary layer model, although the boundary layer equations are not solved in this analysis. Instead, correlations developed either from data or from boundary layer calculations are used to provide, for example, the convective heat transfer coefficient for the heat balance that determines the regression rate. The effect of heat transfer by radiation can also be included. Such models were employed in the present program as a basis for thrust chamber design calculations.

Several years ago, Green[20] reviewed many of the one-dimensional models used to predict burning rate as a function of axial position along the grain of a solid rocket motor. As noted earlier, some of these models assume that the rate-controlling process is the rate of heat transfer from the cross flow to the solid propellant. In other models the rate-controlling process is the rate of diffusion of oxygen through the gas film next to the surface. Green found that such simple models provide results in good agreement with available data. The application of one-dimensional models requires knowledge of suitable heat or mass transfer coefficient correlations. Generally, the axial variation of mean values of the cross, or axial, flow velocity, temperature, etc., can be estimated by integrating the one-dimensional gas dynamic equations. Also, for simple port geometries the effect of port area variation on gas conditions is readily estimated. Thus, one-dimensional analyses provide means for rapidly estimating the burning rate in the hybrid rocket combustor. However, for complex port geometries, it is difficult to use one-dimensional analyses to determine local variations in burning rate around the periphery of the port. Also, heat transfer coefficient correlations are available only for the simplest geometries and limited ranges of flow conditions. Finally, no papers were located that discussed the effects of two-phase flow on the burning rate; the oxidizer is always assumed to be in the gaseous state.

A.2 MULTI-DIMENSIONAL ANALYSES

In recent years, there has been much progress in both analytical methods and computational speed so that two- and three- dimensional computational fluid dynamics (CFD) analysis of complex flow fields can provide useful information for the user with reasonable expenditure of effort and computer resources. Information can be provided by CFD that is either too expensive or too difficult to obtain experimentally. Also, CFD can be used to provide information analogous to experimental results from which simple correlations can be developed for use in design procedures; for example, CFD can be used to develop heat transfer coefficient correlations for flows within complex port geometries.

Except for the oxidizer spray formation process, models exist that provide reasonable estimates of the effects of each of the processes noted above, and these models have been used in various CFD analyses for some time. However, no papers have been published in which a multi-dimensional analysis has been applied to the flow within the hybrid rocket. Analyses of solid-fueled rockets, ducted rockets and solid-fueled ramjets have been published and these methods are now discussed briefly. In such cases, the CFD analysis is coupled to the chemical processes occurring within the solid fuel. The flow field analysis provides the heat transfer rate to the fuel. In some cases, a separate, one-dimensional analysis is used within the grain to determine the local temperature distribution and pyrolysis rate. The mass efflux from the fuel then provides a mass transfer boundary condition to the CFD analysis. Mass transfer also reduces the convective heat transfer rate to the surface so that the entire procedure can be iterative.

For the portion of the flow in which flow recirculation is important (e.g., the head end of the combustor), it is necessary to solve the Navier-Stokes equations in which all of the viscous terms are retained. One of the more popular methods used for solving these equations for subsonic flows is the TEACH procedure outlined in detail in the book by Patankar.[21] In this method, the Reynolds- or Favre(mass)-averaged equations of motion are solved using a control volume formulation. A special procedure is used to compute the static pressure distribution so that the continuity equation is satisfied locally as well as globally.

Cherng et al.[22] applied a two-dimensional TEACH code to the analysis of a ducted rocket. The side-mounted inlets dump air into the combustor at a large angle so that flow recirculation may occur. The solid fuel provides a gas flow mass transfer boundary condition to the cross (main) flow. There is no second phase in the main flow. A two-step kinetics model is used (fuel --> CO, CO --> products). The rates of reaction are computed using an eddy breakup model. The same authors subsequently applied a three-dimensional TEACH code in the study of ducted rockets.[23] Nabity[24] applied a similar

method to compute the flow within a solid-fueled ramjet combustor. A different numerical method has been used by Sabnis et al.[25] to provide a cold flow simulation for flows in a solid-fueled rocket.

Acurex Corporation is using the KIVA computer program[26] for modeling hybrid rockets. The code has also been used by Acurex to compute flow fields in rocket combustion chambers and nozzles, to model rocket exhaust plumes, and to simulate the reacting (dissociating) flow around vehicles in hypersonic flight. For example, KIVA is being used to determine the initial distribution of oxygen that results in uniform burning of the grain. The KIVA code solves the time-dependent form of the governing equation for two-phase, three-dimensional flows within a moving coordinate system the code was developed originally for modeling flows within Diesel engines. As demonstrated by Acurex, KIVA, with suitable modeling assumptions and code modifications, can be used to analyze the flow within hybrid rockets.

Presently, Acurex uses the Solid Propellant Rocket Motor Performance Prediction computer program (SPP)[27] to compute the burning rate, which is then provided to KIVA as a boundary condition. At each instant of time, the SPP code is used to provide a burning rate. KIVA is then used to estimate the new flow field and grain boundary. The cycle is then repeated for the next time instant. Since the grid system can move in the KIVA program (recall that it was developed originally for Diesel engine modeling), it is also possible to integrate the SPP and KIVA codes to provide a direct simulation of the grain burning process.

The SPP code is essentially a modular, comprehensive, one-dimensional code for predicting the performance of solid-fueled motors. However, nozzle performance is computed using a method of characteristics analysis and a boundary layer loss correction procedure. The program consists of several modules:

- Master control module
- One-dimensional equilibrium module

- One-dimensional kinetics module
- Grain design module
- Standard stability performance module
- 2D-two phase nozzle module
- Boundary layer module for nozzle losses due to viscous effects
- Post-processing module.

Note that detailed flow field information within the combustion chamber cannot be obtained from this code, since the flow within this region is treated as one-dimensional.

Both the KIVA and TEACH codes have been used to model two-phase flows in combustors (see, for example, reference 28).

If flow recirculation is not important in the axial direction, then the governing equations are simplified greatly and the computational effort is reduced substantially. In this case, it becomes possible to use a so-called space-marching technique in which the solution is advanced in the axial direction. Secondary flows in the cross planes can be modeled. For the hybrid rocket motor, the flow distant from the grain port entrance is largely axial. (Note that the presence of a second phase (e.g., droplets) can still be accommodated in space-marching codes.) Generally, the governing equations are reduced to either the boundary layer equations or a somewhat more complicated form; in either case, gradients of viscous stresses in the axial direction are neglected.

Models for solid-fueled rockets and ramjets have been developed using space-marching techniques. Several papers have been published by Professor K. K. Kuo based on the solution of the turbulent boundary layer equations for two-dimensional, planar or axisymmetric, flow.[29-33] A one-dimensional heat transfer analysis in the direction normal to the grain surface is also employed. The solutions for the two phases are coupled by (say) the unknown temperature at the surface. An extremely detailed description of such a model is given in reference 29. The governing equations for the gas phase are

Reynolds-averaged. Details of the derivation of the turbulent kinetic energy (k) and dissipation rate (epsilon) equations are provided. In the solid, the one-dimensional form of the steady-state heat conduction equation is solved using the burning rate as the "convection" velocity. The fuel burning rate in the gas phase is described by a one-step eddy breakup model. The burning rate in the solid phase is given by an Arrhenius reaction rate expression. Coupling of the two phases is provided by the unknown surface temperature. Details of the boundary conditions are given, including the special forms for k and epsilon. The parabolic form of the gas phase equations is solved using the Patankar and Spalding method.[34] Details of code development and verification are also given. A special Couette flow analysis is used in the near-surface region.

Godon et al.[35] used a similar approach in a study of erosive burning in solid rockets. Patankar and Spalding's boundary layer method[34] was used to compute the core flow. The inner flow (near wall) region is solved using a Couette flow model. The local burning rate is an eigenvalue which is iterated to permit matching the flow solutions for the two models. The local burning rate is presumed at each axial location and then the Couette flow is computed using the burning rate as a mass transfer boundary condition. The burning rate is then adjusted until the solutions from the Couette flow model and boundary layer analysis agree where the two flow regions merge.

Although no papers have been published describing the application of CFD to the analysis of hybrid rocket motors, it is evident from the available literature that CFD has been used in a variety of combustion systems. Except for the effects of the moving boundaries (i.e., the grain surface regression), the combustor flow fields analyzed are essentially as complicated as those encountered in a hybrid rocket. Since the time-scale for consumption of the solid fuel is on the order of tens of seconds, it is possible to use CFD codes to obtain the instantaneous regression rate distribution. Direct coupling of the motion of the surface to the computation of the flow field is not necessary, although it may be convenient to do so. For the foreseeable future, application of CFD codes to model the head-end of the hybrid combustor can

best be done by the CFD specialist. However, application of a space-marching CFD code to model the three-dimensional, axial-flow portion of the flow field can be made by users familiar only with the use boundary-layer codes. Direct extension of codes used for solid propellant motors requires the addition of (1) a model for the transport of a second phase and (2) a model for combustion in the gas phase. For existing models applicable to solid-fueled ramjets, the gas-phase combustion model is essentially unchanged. In either case, code modifications are straightforward.

Appendix B
OXIDIZER INJECTION TECHNOLOGY

Elemental oxygen is the oxidizer of choice for a large hybrid booster. Hence, attention was focused in this program on means of introducing elemental oxygen into the hybrid combustion chamber. This oxidizer can be injected in either the liquid or the gaseous state and, in preliminary considerations of the alternatives, there appear to be valid arguments favoring each of these approaches. For example, use of liquid oxygen (LOX) fosters minimization of plumbing volumes and system response times. Also the effective gas velocities at the head end of a hybrid rocket engine can be controlled by prolonging the vaporization so that it occurs along the length of the port. On the other hand, LOX injection into the hybrid grain port could cause, through droplet impingement, grain surface erosion and/or reaction quenching. Furthermore, appropriate control of the LOX atomization process could necessitate a costly injector having a large number of spray elements, a large injection pressure drop that is disadvantageous from the standpoint of pump work requirement (system performance), and/or a large free volume for vaporization upstream of the fuel grain (with attendant motor mass fraction depreciation). While most of these potential LOX disadvantages would be obviated by injection of gaseous oxygen (GOX), the benefits would come at the cost of increased plumbing weight and volume as well as somewhat reduced system control responsiveness and potentially heightened detrimental coupling of the feed system with the combustion process.

In order to provide a rational basis for selecting between the fluid injection alternatives, efforts in the present program were directed to (1) a trade study of oxygen injection techniques applicable to hybrid booster designs, with a view toward selection of a preferred injection technique; (2) a determination of the nature and scope of the criteria and databases available to guide implementation of the preferred injection technique(s); (3) baseline specification of LOX injector characteristics for hybrid booster motors; and (4) development of a technology plan to eliminate identified deficiencies in the existing databases.

B.1 LIQUID OXYGEN INJECTION

The following issues were addressed in regard to LOX injection into the dome of the hybrid rocket:

- Identification of important spray parameters
- Identification of candidate injector geometries
- Determination of injector sizing and layout
- Development of a plan to obtain deficient injector design technology.

Each issue is treated in turn in the following discussion.

B.2 IDENTIFICATION OF IMPORTANT SPRAY PARAMETERS

In order to preclude the possibility of reaction quenching as well as the likelihood of surface erosion that accompany impingement of LOX on the solid fuel surface while delivering the substantial oxidizer mass fluxes implicit in the baseline thrust chamber designs, it seems prudent to vaporize a large percentage of the LOX in the dome before it enters the grain ports. This vaporization could be achieved by using the energy released by the burning solid fuel surfaces facing the dome in combination with that contained in the LOX turbopump exhaust gases.

Calculations were done with a spray vaporization program to determine the maximum droplet size which could be vaporized in a dome configuration representative of a hybrid booster rocket. This spray vaporization program uses a quasi-steady vaporization model and includes the following features:

- Spherical symmetry
- Dilute droplet density
- Convective heat/mass transfer
- Simultaneous droplet heatup and vaporization
- Fluid properties as functions of temperature
- Consideration of vapor blocking.

Calculations were made to determine the effect of the dome length and droplet velocity on the vaporization of a droplet. The thrust chamber operating pressure was assumed to be 750 psia, and the dome temperature was assumed to be at 1500°R as a consequence of the burning of the front face of the solid fuel ports and the injection of the hot turbine exhaust gas into the dome.

Figure B-1 shows the calculated effect of droplet size on the length for complete vaporization. As expected, the length for complete vaporization increases with increasing droplet size. The droplet velocity was 50 ft/sec for these calculations. Figure B-2 shows the effect of droplet velocity on the length required for complete vaporization. Increasing the droplet velocity is also seen to increase the length required for complete vaporization.

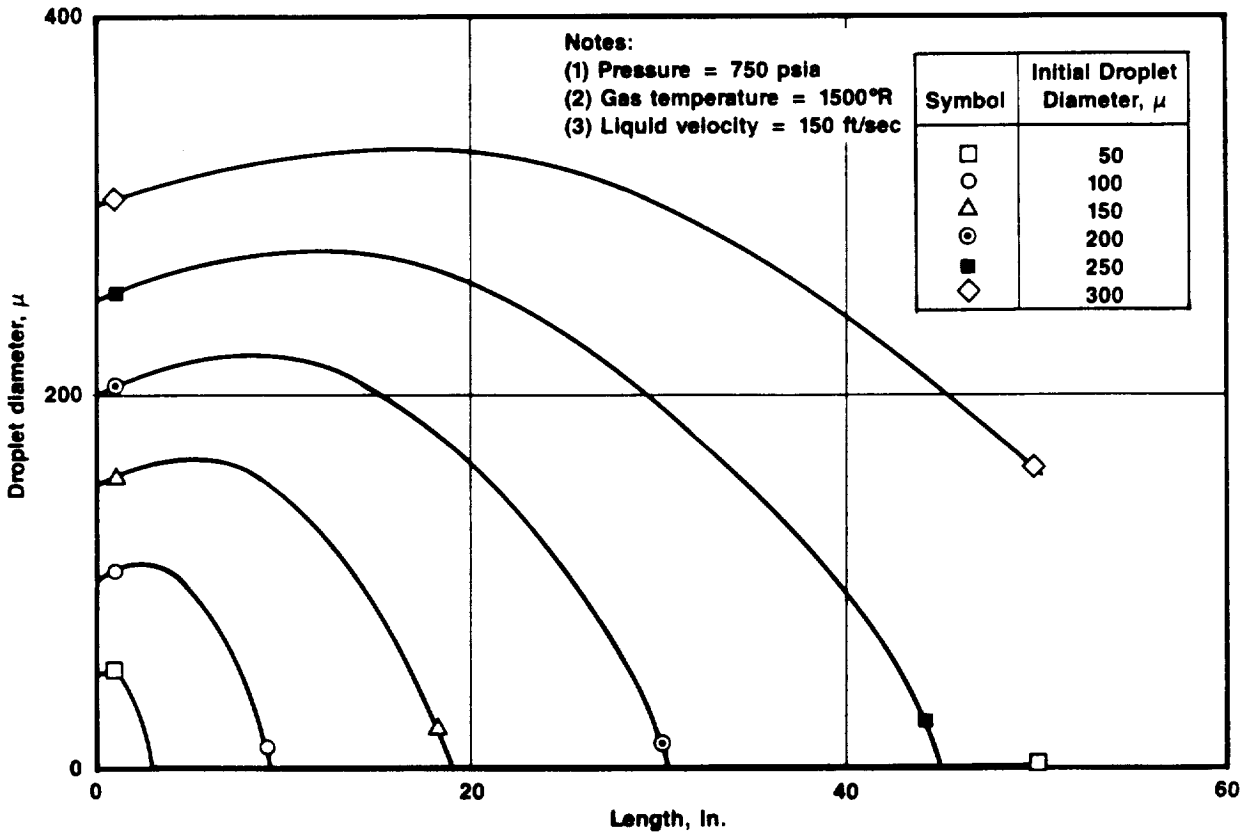

Figure B-1. Longer Length is Required for Complete Vaporization as Initial Droplet Size Increases

50436

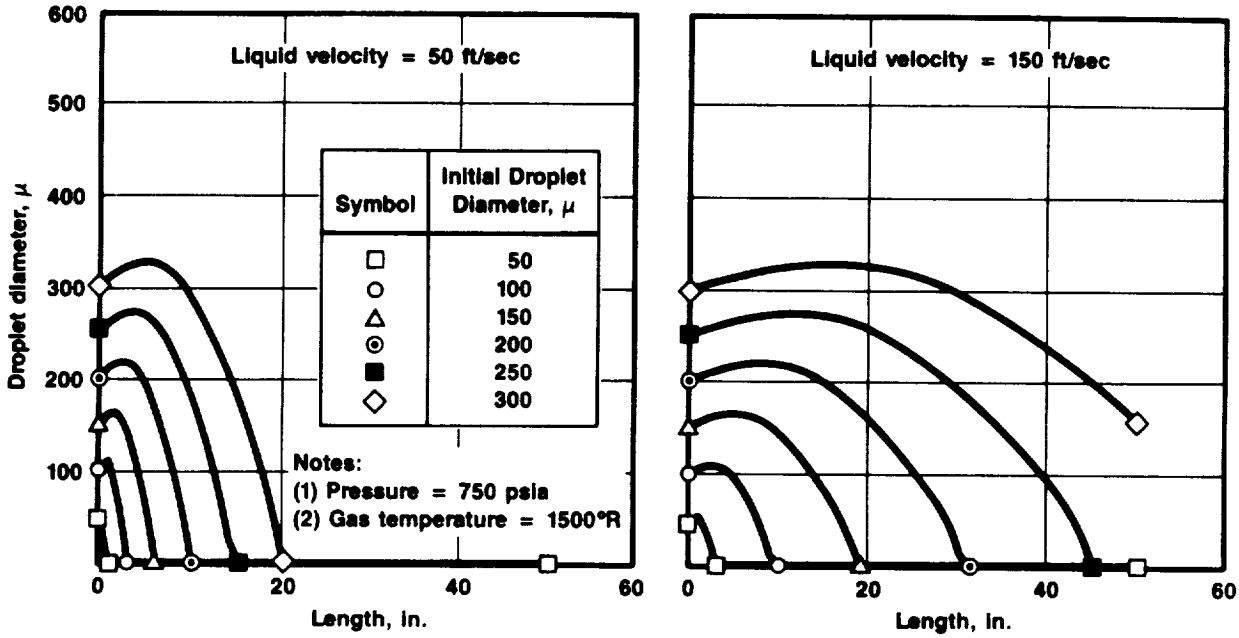

Figure B-2. Longer Length is Required for Complete Vaporization as Liquid Velocity Increases

50437

A correlation was generated from these calculations which relates maximum droplet size for complete vaporization to dome length and liquid velocity, viz:

$$\text{Maximum droplet size} = 502.7\ (V_L)^{-0.62} * (L_V)^{0.64} \qquad \text{(B-1)}$$

where

V_L = liquid velocity, ft/sec
L_V = vaporization length, in.

Consonant with baseline cycle analyses for the hybrid rocket, the maximum pressure drop across the injector was limited to 212 psi. This pressure drop translates into an injector exit velocity of 167 ft/sec. Using Equation (B-1), the largest droplet size that could be vaporized in a distance representative of that available in a booster dome, say 20 in., is 145 microns.

Thus, if complete vaporization is required in such a dome prior to port entrance, injectors must be sized so that the largest droplet produced is 145 microns.

Injectors generate a range of droplet sizes (i.e., a distribution) and are usually characterized by some mean droplet size, such as a Sauter mean diameter (SMD). (The SMD is the ratio of the sum of the volume of all the droplets to the sum of the surface area of all the droplets in a spray.) Therefore, it is useful to relate the calculated maximum droplet size to the SMD.

Spray droplet size distribution is commonly described in terms of the Rosin Rammler distribution. The form of this distribution is

$$1 - q = \exp(-(d/x)^N) \qquad \text{(B-2)}$$

where

q = fraction of liquid volume having droplet sizes less than d.
X = mean diameter, microns.
N = measure of the spread of the distribution.

The SMD of a Rosin Rammler distribution can be calculated by the following equation:

$$SMD = X/\Gamma((N-1)/N) \qquad \text{(B-3)}$$

where $\Gamma()$ = Gamma function

Therefore, if the X and N parameters are known, the droplet size distribution and the SMD are known. The SMD can then be related to the largest droplet size in the distribution. The largest droplet size of a distribution is defined as that which is reached after 99.9% of the total liquid volume has been accounted for by summing the volumes of all smaller droplets in the distribution. Figure B-3 gives a plot relating the maximum droplet size to SMD for an N of 2.

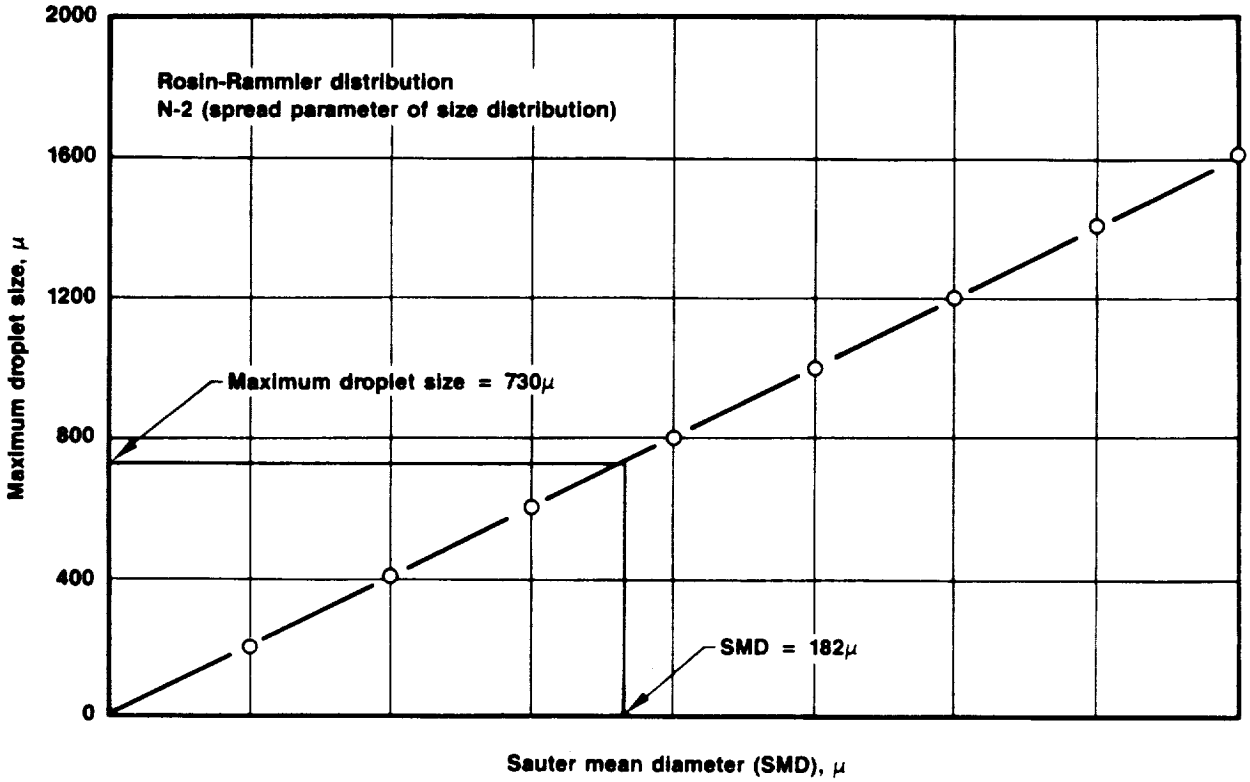

Figure B-3. Sprays Having a Small Sauter Mean Diameter Still Contain Large Droplets

50438

Use of Equations (B-1), (B-2), and (B-3) allows the calculation of the SMD that will result in complete vaporization within a prescribed length. If complete vaporization is not desired, Equation (B-4) can be used to approximate the SMD that will achieve the desired amount of vaporization. Equation (B-4) comes from the assumption that vaporization follows a droplet-diameter-squared functionality.

$$\text{SMD}(\%\ \text{vaporization}) = \frac{\text{SMD}(100\%\ \text{vaporization})}{\text{SQRT}(1-(\%\text{liquid})^{0.66})} \qquad \text{(B-4)}$$

Therefore, the maximum allowable mean droplet size can be calculated using Equations (B-1), (B-2), (B-3), and (B-4) for a given distance between the injector and the port entrances, for a desired degree of vaporization at the port entrances, and for a given droplet size distribution. If droplet size

distribution information were available as a function of injector type/size and operating conditions, then injectors could be sized to generate sprays having the maximum allowable mean droplet size.

B.3 EVALUATION OF CANDIDATE INJECTION ELEMENTS

Two injector element types were identified as possible candidates for use in a hybrid rocket combustor based on past gas turbine and rocket injector experience:

- Like-on-like impinging injector
- Pressure-swirl injector with and without gas assist.

A like-on-like impinging injector uses the impingement of two or more injectant streams to atomize the liquid. A pressure-swirl injector without gas assist uses centrifugal forces to form a thin conical sheet of liquid that can readily be disintegrated (i.e., atomized). With gas assist a small amount of high velocity gas exits the injector axially and impinges on the liquid sheet to assist in the atomization process. The pressure-swirl element with or without gas assist should produce smaller droplet sizes than a like-on-like impinging element for a constant liquid flow rate and pressure drop. This expectation is based on the fact that the characteristic dimension for atomization with a pressure-swirl injector with or without gas assist is the sheet thickness, which should be significantly smaller than the characteristic dimension of the like-on-like impinging injector (i.e., the liquid jet diameter). Further considerations bearing on the performance and applicability of these element types are discussed in Appendix C and references 1 through 10.

B.4 INJECTION ELEMENT SIZING AND LOCATION

Once the element type to be used as the basis for this analysis of a LOX injection system had been selected, attention then turned to establishment of a basis for sizing the elements and establishing their placement in the thrust chamber dome. Again, the use of energy contained in turbopump exhaust gases to accelerate droplet vaporization within the dome and the need to produce a

uniform gaseous oxygen distribution at the port entrances were assumed. Figures B-4 through B-6 give possible hybrid booster injector configurations.

Figures B-4 and B-5 show injectors having elements evenly distributed over the chamber cross-section to promote uniform oxygen distribution. Two manifolds are used, with the turbopump exhaust gas and the liquid oxygen going to separate manifolds. In Figure B-4 the exhaust gas is bled into the dome

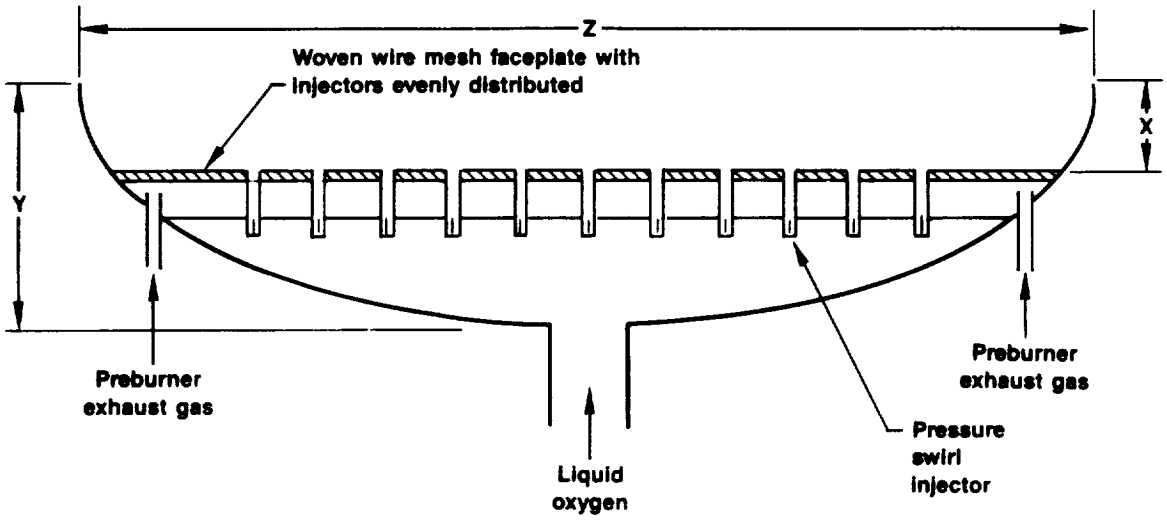

Figure B-4. Injector Configuration No. 1

50439

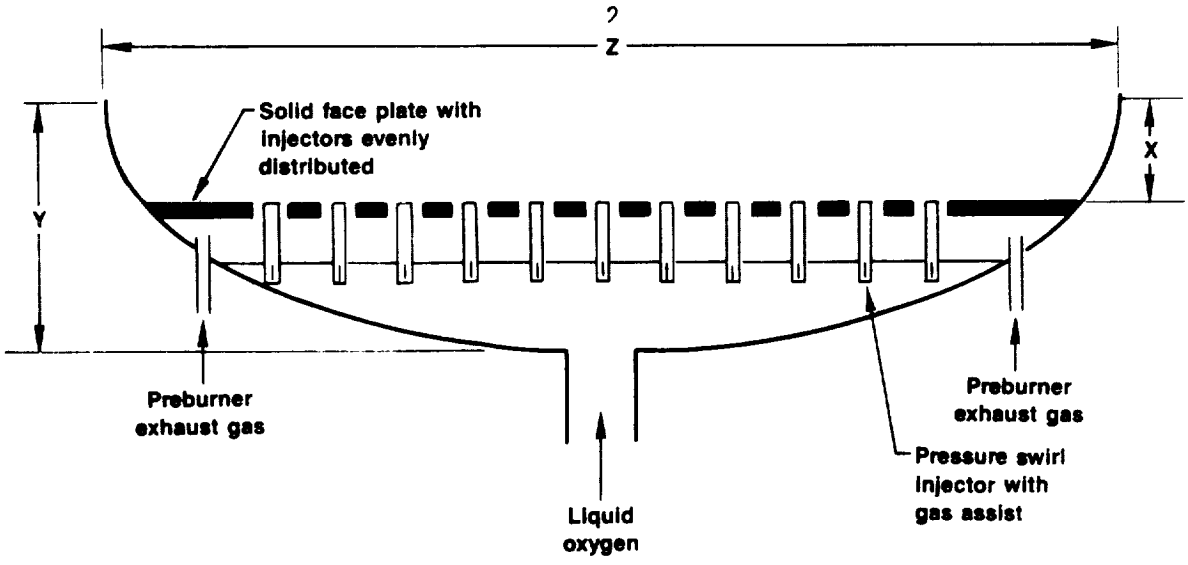

Figure B-5. Injector Configuration No. 2

50440

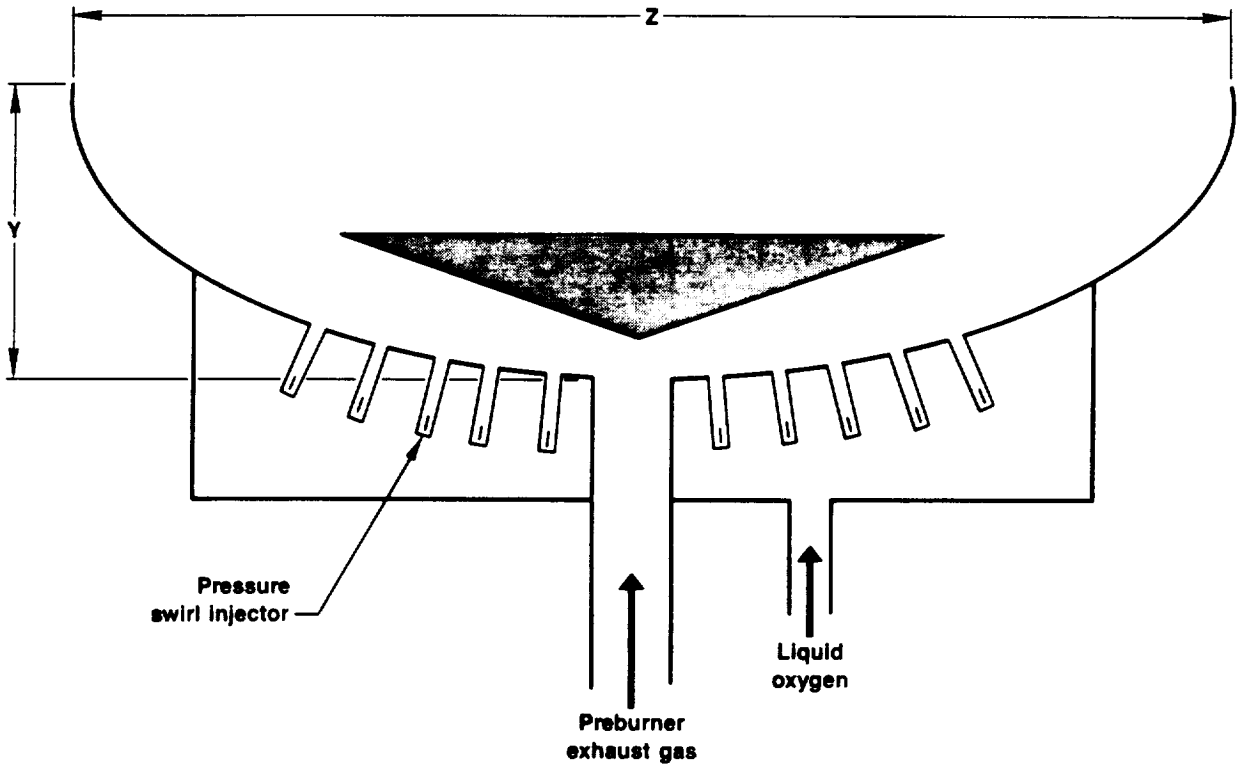

Figure B-6. Injector Configuration No. 3

50441

through woven wire mesh material. The pressure drop across this woven wire mesh material would be low, and the material can be used with hot gases at temperatures up to 1500°F to 1650°F. The liquid would be injected into the dome with through pressure-swirl elements.

The injector of Figure B-5 is similar in configuration except that the woven wire mesh material is replaced by a solid wall and the preburner exhaust gas enters the dome through annular gaps surrounding the liquid injection elements. If a sufficiently high gas momentum can be achieved, this approach offers the advantages of the gas assisting the atomization process, the gas/liquid mixing process, and the vaporization process.

Figure B-6 shows an approach in which the liquid is injected into the turbine exhaust gas directly. This offers the best liquid/exhaust gas contact, but could present difficulties with respect to achieving a uniform gaseous oxygen distribution at the port entrances.

TABLE B-1. HYBRID BOOSTER DESIGN INFORMATION

T17046

Parameter	Engine Designation			
	A	B	C	D
Engine diameter, m (in.)	4.57 (180)	4.57 (180)	2.44 (96)	2.44 (96)
Dome length, m (in.)	1.32 (52)	1.32 (52)	0.71 (28)	0.71 (28)
Maximum oxygen mass flow rate, kg/s (lb/sec)	3904 (8600)	2497 (5500)	953 (2100)	636 (1400)

Table B-1 gives the important parameters for several hybrid rocket designs. Injector sizes for these various engines were determined according to an assumed requirement for a given percentage of LOX vaporization upstream of the grain port entrances. It was assumed for this analysis that the distances available for vaporization (i.e., the X dimension in Figures B-4, B-5, and B-6) are 40 in. and 20 in. for the large and small rocket engines, respectively. These distances are reasonable in view of the likely geometry of the domes and the need, in each case, to reserve volume for injectant manifolding. The results of analysis performed to date indicate that complete vaporization of the liquid mass in these distances would require a very large number of injectors (i.e., in the 10,000 range). Also, it was decided that the injector sizing should be done at the lower end of the anticipated turndown range to ensure that the majority of the liquid would be vaporized over the entire mission. Therefore, it was decided to size the injectors so that 70% of the liquid would be vaporized at the port entrance for a liquid flow rate that is 75% of the maximum liquid flow rate. This criterion is, of course, a "current best estimate" and would need to be verified during Phase 2 activities.

Table B-2 gives the results for the small rocket engine. The determined injector element orifice diameter was 0.2 in. It can be seen that at the port entrances 83, 70, and 65% of the liquid is vaporized at flow rates that are 100, 75, and 65% of the maximum flow rate.

TABLE B-2. INJECTOR SIZED SO THAT 70% OF LIQUID IS VAPORIZED IN 1.02 M (40 IN.) AT A FLOW RATE OF 75% OF MAXIMUM FLOW RATE (LARGE BOOSTER)

T17047

Maximum flow, %	100	75	65
Mass flow/injector element, kg/s (lb/sec)	1.59 (3.5)	1.18 (2.6)	1.04 (2.3)
Predicted SMD, m (in.)	1.75 (69)	2.36 (93)	2.69 (106)
Maximum SMD for 100% vaporization, m (in.)	1.52 (60)	1.75 (69)	1.98 (78)
% vaporized	88	70	69

Note: injector diameter = 0.0107 m (0.42 in.)

TABLE B-3. INJECTOR SIZED SO THAT 70% OF LIQUID IS VAPORIZED IN 0.51 M (20 IN.) AT A FLOW RATE OF 75% OF MAXIMUM FLOW RATE (SMALL BOOSTER)

T17048

Maximum flow, %	100	75	65
Mass flow/ injector element, kg/s (lb/sec)	0.37 (0.82)	0.28 (0.62)	0.24 (0.53)
Predicted SMD, m (in.)	1.22 (48)	1.65 (65)	1.85 (73)
Maximum SMD for 100% vaporization, m (in.)	1.02 (40)	1.22 (48)	1.32 (52)
% vaporized	83	70	65

Note: injector diameter = 0.0051 m (0.2 in.)

Table B-3 gives the results for the large rocket engine. The determined injector element orifice diameter was 0.42 in. It can be seen that at the port entrances 88, 70, and 69% of the liquid is vaporized at flow rates that are 100, 75, and 65% of the maximum flow rate.

Based on these injector sizes, the number of injector elements required for each rocket engine configuration can be calculated. The results of such calculations can be seen in Table B-4. The number of injector elements for all engines is in the neighborhood of 2000. (The smaller engines require roughly the same number of injectors because the vaporization distance is shorter for the smaller rocket engine configurations.) This number of elements is consistent with current design practice for large liquid propellant rockets, but it appears inconsistent with the reliability and cost objectives of the hybrid booster concept. Furthermore, it is inconsistent with previous experience at CSD in hybrid testing. Past designs have not used more than four injectors for a single-port test and not more than one per port in multi-port tests. These discrepancies indicate a need for further study in this area.

TABLE B-4. NUMBER OF INJECTOR ELEMENTS DETERMINED BY LOX FLOW RATE

T17049

Parameter	Booster Size	
	Small	Large
Injector diameter, m (in.)	0.0051 (0.2)	0.0107 (0.42)
Vaporization length, m (in.)	0.51 (20)	1.02 (40)
No. of injector elements		
Engine A		2400
Engine B	2500	
Engine C		1550
Engine D	1700	

B.5 GASEOUS OXYGEN INJECTION

Gaseous oxygen injection eliminate the need for liquid breakup and vaporization in the limited space of the dome. Therefore, the injectors and dome need to be designed to generate only a flow field which results in uni-form gaseous oxygen distribution to the solid fuel ports. In contrast to the situation for the liquid injection processes, the state of the art currently applicable to the design of gaseous oxygen injectors includes reliable numerical procedures for sizing and locating injector elements so as to promote uniform flow distribution among the several ports of a hybrid booster grain. Computer codes (e.g., TEACH and KIVA) having capabilities to handle steady and non-steady, three-dimensional, reacting, recirculating flows are currently operational and available for analytical modeling of the dome of the hybrid motor employing a gaseous-oxidizer injector design.

The three-dimensional TEACH code is one of the more popular methods for solving the Navier-Stokes equations for subsonic flows. This method is outlined in detail in a book by Patankar.[11] In this method, the Reynolds- or Favre(mass)-averaged equations of motion are solved using a control volume formulation. A special procedure is used to compute the static pressure distribution so that the continuity equation is satisfied locally as well as globally. The KIVA code[12] solves the time-dependent form of the equations representing three-dimensional flows. The efficacy of both of these codes has been demonstrated in application to analysis of flow fields as complex as those likely to occur in the dome of hybrid boosters. This builds confidence

in their potential utility for hybrid injector design, but efficacy in this particular application has yet to be verified. Additional details on numerical codes available for modeling flows in the dome of the hybrid rocket are discussed in subsection 2.2.1 of this volume.

Because of the unknowns of using liquid injection of oxygen for a hybrid booster system, the baseline selection for the oxygen feed system was one based on GOX (see Volume I). However, a final judgment must be reserved until Phase 2 efforts have confirmed the anticipated benefits of the Acurex pumping system and clarified, in terms of the effects on grain regression behavior and overall engine operability, the advisability and required extent of oxidizer prevaporization. Further, the final selection of an injection approach should be based on a somewhat more advanced injector design technology than is currently available. For example, more droplet size data are required before pressure-swirl injectors, with or without gas assist, can be accurately designed to generate sprays with desired mean droplet sizes and droplet size distributions. Also, the applicability of extant numerical flow field analysis codes to the design of gaseous oxygen injectors having multiple elements servicing multiple grain ports needs to be verified. Hence, it is recommended that technology advancement studies be directed toward improved and extended characterization of pressure-swirl injection elements as well as flow visualization and analysis studies pertinent to the design of gaseous injectors be undertaken in Phase 2 of the program.

Appendix C

INJECTOR ELEMENT SELECTION CONSIDERATIONS

To support the injector element selection process, the following sections will discuss the advantages and disadvantages of two candidate injector element types, namely, impinging-jet and pressure-swirl configurations.

In terms of fabrication effort the like-on-like impinging injector is probably the simplest to fabricate. Pairs of orifices need to be drilled for this injector configuration. The major difficulty is that these orifices must be drilled in such a way that the liquid streams impinge exactly. The fabrication of a pressure-swirl injector also offers challenges. The liquid exiting a pressure-swirl injector is swirling and therefore some means of developing this swirl must exist. P&W-GEB uses three tangential slots in the end of a tube to generate the swirl for their rocket combustor pressure-swirl injectors. These tangential slots in the end of the tubes probably make the fabrication process of this injector configuration more difficult than for the like-on-like impinging injector configuration. Pressure-swirl injectors used in gas turbine combustors and oil burners have swirl chambers into which the liquid enters through tangential slots. The diameter of this swirl chamber is larger than the injector exit diameter. This injector configuration would be even more difficult to fabricate.

These two injector configurations have different spray shapes. The like-on-like impinging injector has a solid fan shape and the pressure-swirl injector has a symmetric hollow cone shape. Due to the small droplet sizes necessary to achieve the desired degree of vaporization before the port entrances, a large number of small injectors will be necessary. Consequently, the shape of the spray is probably not an important consideration in the injector selection process if vaporization is achieved before the spray reaches the grain. If a major portion of the vaporization occurs in the fuel ports, the pattern will be important as quenching may occur with the hollow cone pattern.

Ferrenberg, et al.[R1] recently has reviewed earlier experimental work to determine the spray characteristics of like-on-like impinging injectors as well as other rocket injectors. He concluded the following:

- Experimental fluid properties and flow conditions were generally far from those of a rocket injector.
- Existing correlations were empirical and can't be extended with much confidence beyond the variable range over which they were developed.
- Earlier measurement techniques had problems which resulted in data of questionable accuracy.

Equation (C-1)[2] is the correlation most often used to predict droplet sizes of a like-on-like impinging injector:

$$MMD = 1.6x10^5 \ (V_L)^{-1}(d_j)^{0.57}(P_c/P_j)^{-0.1} * K_{prop} \qquad (C\text{-}1)$$

where

MMD = mass median diameter (i.e., 50 % of the liquid mass have droplet sizes smaller than the MMD), microns
V_L = liquid velocity, ft/sec
P_c = dynamic pressure at center of jet
P_j = mean dynamic pressure of jet.

This correlation was developed from droplet size data using hot wax sprayed into air. It was concluded in reference 1 that data obtained using this technique are questionable. The orifice sizes tested ranged from 0.04 in. to 0.08 in. The jet liquid velocity ranged from 30 ft/sec to 220 ft/sec.

Since only hot wax was used as the liquid, no property variation was investigated. The Kprop term resulted from a different study,[3] which involved experiments with cross current injection of single streams into flowing gases. Its applicability to co-current injection is questionable.

Brault and Lourme[4] have recently investigated sprays generated by like-on-like impinging injectors with a Malvern Droplet Size Analyzer over a range of liquid properties, liquid mass flow rates, chamber densities, and injector sizes. The orifice sizes investigated ranged from 0.08 in. to 0.12 in. The liquid jet velocity ranged from 66 ft/sec to 131 ft/sec. A limited number of liquid property variations and chamber pressure/density variations were also investigated. Equation (C-2) is the correlation which resulted from this investigation.

$$MMD = 1.3*(V_L)^{-1}*(d_j)^{0.3}*(\rho_G)^{-0.15}*(\sigma)^{0.5} \qquad (C\text{-}2)$$

where

MMD = mass median diameter, microns
V_L = liquid velocity, mps
d_j = liquid orifice diameter, mm
ρ_G = chamber density, kg/m^3
σ = liquid surface tension, kg/s^2

Hautman[5] has also recently investigated like-on-like impinging injectors with a Malvern droplet size analyzer. The variation in liquid properties, liquid flow conditions, and chamber pressures/densities was much larger in this investigation than any other investigation. However, injector orifice size was mainly limited to a diameter of 0.08 in. Equation (C-3) was the correlation which resulted from this investigation.

$$SMD = 1.29x10^{7}*((\rho_L)*(V_L)^2)^{-0.7}*(\sigma)^{0.59}*(\rho_G)^{-0.09} \qquad (C\text{-}3)$$

where

SMD = Sauter mean diameter, microns
V_L = liquid velocity, mps
ρ_L = liquid density, kg/m^3

Review of these correlations and the conditions over which they were developed indicates that correlations do not exist to adequately predict the mean droplet size or the spread of the droplet size distribution over a wide range of operating conditions and sizes. The prediction of a mean droplet size is possible for certain size injectors, but the effect of the orifice diameter on the mean droplet size has not been well established. The effect of liquid properties and chamber density on the mean diameter has been investigated and is taken into account in Equations (C-2) and (C-3). However, no information exists which would allow the prediction of the spread of the distribution, which is needed to determine the largest droplet sizes.

A significant amount of research has been directed towards the pressure-swirl injector with and without gas assist. Fraser, Dombroski, and Routley,[6] Simmons,[7] and Ingebo[8] investigated pressure-swirl injectors with gas assist. These studies used very small injectors, low liquid and gas flow rates, and low chamber pressures. This work was also done before the advanced laser droplet sizing techniques were available.

A large amount of work has also been done with pressure-swirl injectors without gas assist. Some of the most recent work is that of Lefebvre,[9] who used a Malvern droplet size analyzer. Equation (C-4) is the correlation that he developed.

$$SMD = 2.25*(\sigma)^{0.25}*(\mu)^{0.25}*(\dot{m}_L)^{0.25}*(\Delta P_L)^{-0.5}*(\rho_G)^{-0.25} \qquad (C\text{-}4)$$

where

μ = liquid viscosity, kg/m-s
ΔP_L = liquid pressure drop, Pa
$\dot{m}_L$ = liquid mass flow rate, kg/s

Hautman[10] attempted to determine the spray characteristics of a pressure-swirl injector with and without gas assist with fluid properties and flow conditions similar to those of a rocket combustor. The sprays generated

at typical rocket combustor conditions were found to be very dense and presented severe difficulties for laser-based droplet sizing instrumentation, such as a Malvern droplet size analyzer. However, the data presented in reference 5 are the only data available for pressure-swirl rocket injectors with and without gas assist at the larger sizes and at conditions close to the actual conditions. The correlation that was developed is given in Equation (C-5):

$$SMD = 2.55x10^{5}*(1+((\dot{m}_G*V_G)/(\dot{m}_L*V_L)))^{2}*(\rho_G)^{0.35} *(\sigma)^{0.44}*(\rho_L)^{0.29}*(\Delta P_L)^{-0.59}*(AR)^{-0.34} \quad \text{(C-5)}$$

where

$\dot{m}_G$ = gas mass flow rate, kg/s
V_G = gas velocity, m/s

Since the liquid swirl plays a major role in determining the spray character, the slot to tube area ratio was included in Equation (C-5). This term accounts for the effect of the injector geometry on the swirl generation process.

The effect of chamber density, liquid properties, and liquid and gas flow rate for a fixed geometry seem to be fairly well established and the correlations reported by Hautman[10] or Lefebvre[9] could be used to determine these effects. However, none of the above investigations tested large injectors with large liquid flow rates. Hautman tested large injectors, but at reduced liquid flow rates due to droplet sizing instrumentation limitations at the higher liquid flow rates. Even at the reduced flow rates the droplet sizing instrumentation was being pushed to its limit. Therefore, additional work is required before one can accurately design pressure swirl injectors with or without gas assist to generate sprays with the desired mean droplet size and droplet size distribution.

Appendix D
OPTICAL INSTRUMENTATION

Advanced diagnostics are available to facilitate temperature and species measurements in hybrid rocket combustion experiments. In the recommended slab burner studies, it is necessary to perform measurements remotely and unobintrusively -- conditions which recommend optical and laser diagnostics. The hostile conditions, high temperatures, and need to avoid perturbation or chemical contamination of the flow prohibit use of physical probes such as thermocouples or gas sampling probes.

A Malvern droplet size analyzer and an Aerometrics phase-doppler particle analyzer are conventional, commercially available instruments that are based on mature technologies and are available for use in the characterization studies. Other advanced laser diagnostic techniques are available, and the Laser Diagnostics group at UTRC has all the necessary equipment including Nd:YAG, argon, and excimer lasers, 1-D and 2-D detectors, and the experience required to implement them for these tests. Some of these diagnostics are mature and have been demonstrated in a test stand; others are still under development, but would have a high payoff for the proposed program if their development proceeds rapidly enough.

Coherent Anti-Stokes Raman Spectroscopy (CARS) is in an advanced state of development and has regularly been employed at UTRC in test stands to observe highly sooting combustion systems. While CARS is generally used for single point measurements, it can measure multiple species as well as gas temperature (Eckbreth and Anderson, 1985)[D-1], as the experimental volume is scanned. It has proven applicable to extremely hostile environments (Stuff-lebeam and Eckbreth, 1989[D-2]; Eckbreth, et al., 1984)[D-3] and to heavily sooting, particle-laden flames by Boedeker and Dobbs (1986)[D-4].

Extremely high particle loadings may result from the metallized fuels proposed for Phase 2 tests and may cause unacceptable levels of scattering and

interference for laser diagnostics. However, particle emissions themselves can be used successfully for temperature measurements through pyrometry (Berger, et al., 1985)[D-5]. Also, photographic techniques have been used for particle sizing and velocity measurements (Kol, et al., 1986)[D-6] in aluminum combustion. Spray and atomization measurements to date have generally used surrogate fluids and conditions rather than LOX itself. Recent developments in the laser diagnostic field support the suggestion that direct measurements on LOX itself may be possible.

Fluorescence techniques have been used for both liquid (Yamagishi, et al., 1981)[D-7] and gaseous oxygen (Lee, et al., 1987)[D-8]. Absorption studies by Dianov-Klokov (1959)[D-9] showed that the liquid oxygen spectrum is dominated by transitions of the (O2)2 complex, sometimes referred to as the singlet oxygen "dimol". In the gas phase, these double molecule complexes are less favorable and the fluorescence is characteristic of just the O2 molecule. The singlet oxygen dimol is easily excited by a Nd:YAG laser (Protz, and Maier, 1980[D-10]; Huestis, et al., 1974)[D-11] and produces emission at 637, 704 and 764 nm. Gaseous O2 is excited with an ArF laser (193 nm) and its fluorescence detected in the Schumann-Runge bands (175-250 nm) (Lee, et al., 1987[D-8]; McKenzie and Laufer, 1988)[D-12].

With further development these two laser systems, together with appropriate two-color detection of the fluorescence, may be able to yield instantaneous maps of the vapor and liquid fields in a spray. Using 2-D detectors and high magnification, individual droplets (approximately 150 microns) may be able to be resolved and tracked. Gas density could also be measured by Rayleigh scattering through measurements similar to Fourguette (1986)[D-13] if particles do not cause interferences. If using conventional sizing instruments becomes problematical other advanced techniques are under development, but are at much earlier stages of development. An alternative for droplet size determination is to employ a nonlinear spectroscopy such as Raman and attempt to use morphology-dependent resonances (MDR's) that should appear in the Raman spectrum (Hill and Benner, 1988[D-14]; Campillo and Lin, 1988)[D-15].

Prior to implementation on the hybrid rocket test stand, the techniques that appear most promising at the time will have to be evaluated for the expected conditions in the laboratory. The laboratory calibration tests will be needed to determine parameters such as absorption coefficients and the spectral resolution necessary for quantitative measurements as well as the degree of accuracy which may be achieved. Phase II experiments will evaluate the techniques mentioned previously to determine the best combination that will yield quantitative measurements from the small-scale tests of injectors and the hybrid fuel combustion experiments.

REFERENCES

D-1. Eckbreth, A. C., and Anderson, T. J., "Dual Broadband CARS for Simultaneous, Multiple Species Measurements," Applied Optics, Vol. 24, pp. 2731-2736, 1985.

D-2. Stufflebeam, J. H., and Eckbreth, A. C., "Multiple Species CARS Measurements of High Pressure Solid Propellant Combustion," Paper No. AIAA-89-0060, pre-sented at the 27th Aerospace Sciences Meeting, Reno, Nevada, January 9-12, 1989.

D-3. Eckbreth, A. C., Dobbs, G. M., Stufflebeam, J. H., and Tellex, P. A., "CARS Temperature and Species Measurements in Augmented Jet Engine Exhausts," Applied Optics, Vol. 23, pp. 1328-1339, 1984.

D-4. Boedeker L. R., and Dobbs, G. M., "CARS Temperature Measurements in Sooting, Laminar Diffusion Flames," Combustion Science and Technology, Vol. 46, pp. 301-323, 1986.

D-5. Berger, M., Fuhs, A. E. and Kol, J., "Two-Color Photo-Pyrometry Method for Temperature Measurement of Moving Burning Particles, Paper No. AIAA 85-0157, presented at the 23rd Aerospace Sciences Meeting, Reno, Nevada, 1985.

D-6. Kol, J., Fuhs, A. E. and Chozev, Y., "Experimental Investigation of Aluminum Combustion in Sulfur Hexafluoride Atmosphere," Paper No. AIAA 86-1334, presented at the AIAA/ASME 4th Joint Thermophysics and Heat Transfer Conference, Boston, MA, June 2-4, 1986.

D-7. Yamagishi, A., Ohta, T., Konno, J., and Inaba, H., "Visible Fluorescence of Liquid Oxygen Excited by a Q-Switched Nd: YAG Laser," Journal of the Optical Society of America, Vol. 71, pp. 1197-1201, 1981.

D-8. Lee, M. P., Paul, P. H., and Hanson, R. K., "Quantitative Imaging of Temperature Fields in Air Using Planar Laser-Induced Fluorescence of O2," Optics Letters, Vol. 12, pp. 75-77, 1987.

D-9. Dianov-Klokov, V. I., "On the Question of the Origin of the Spectrum of Liquid and Compressed Oxygen (12,600 - 3,000A)," Optics and Spectroscopy, Vol. 6, pp. 290-293, 1959.

D-10. Protz, R., and Maier, M., "Laser Induced Fluorescence and Relaxation of Singlet Molecular Oxygen in the Liquid Phase," The Journal of Chemical Physics, Vol. 73, pp. 5464-5467, 1980.

D-11. Huestis, D. L., Black, G., Edelstein, S. A., and Sharpless, R. L., "Fluorescence and Quenching of O2(1@g) and ½O2(Liquid Oxygen," The Journal of Chemical Physics, Vol. 60, pp. 4471-4474, 1974.

D-12. McKenzie, R. L., and Laufer, G., "The Application of Laser-Induced Fluorescence in Airflows to Hypersonic Code Validation," Paper No. 18, Fifth National Aero-Space Plane Symposium, NASA Langley Research Center, October 18-21, 1988.

D-13. Fourguette, D. C., Zurn, R. M., and Long, M. B., "Two-Dimensional Thermometry in a Turbulent Nonpremixed Methane-Hydrogen Flame," Combustion Science and Technology, Vol. 44, pp. 307-317, 1986.

D-14. Hill, S. C., and Benner, R. E., "Morphology-Dependent Resonances," Optical Effects Associated with Small Particles, Barber, P. W. and Chang, R. K., eds., World Scientific, Singapore, pp. 3-61, 1988.

D-15. Campillo, A. J., and Lin, H. B., "Absorption and Fluorescence Spectroscopy of Aerosols," Optical Effects Associated with Small Particles, Barber, P. W., and Chang, R. K., eds., World Scientific, Singapore, pp. 141-199, 1988.

Report Documentation Page

1. Report No.	2. Government Accession No.	3. Recipient's Catalog No.

4. Title and Subtitle
Hybrid Propulsion Technology Program
Volume 1 - Conceptional Design Package
Volume 2 - Technology Definition Package

5. Report Date
9-28-89

6. Performing Organization Code

7. Author(s)
Gordon E. Jensen, Allen L. Holzman, Steven O. Leisch, Joseph Keilbach, Randy Parsley, John Humphrey

8. Performing Organization Report No.
Proj 2027-FR

10. Work Unit No.

9. Performing Organization Name and Address
United Technologies Corporation/Chemical Systems Div.
P O Box 49028
San Jose, CA 95161-9028

11. Contract or Grant No.

13. Type of Report and Period Covered
Final Report for period
March 6, 1989 to Sept 28, 1989

12. Sponsoring Agency Name and Address
National Aeronautics and Space Administration
Washington, D.C. 20546-0001
Marshall Space Flight Center
Huntsville, AL

14. Sponsoring Agency Code

15. Supplementary Notes

16. Abstract

A concept design study was performed to configure two sizes of hybrid boosters - one which duplicates the advanced shuttle rocket motor vacuum thrust time curve and a smaller, quarter thrust level booster. Two sizes of hybrid boosters were configured for either pump-fed or pressure-fed oxygen feed systems. Performance analyses show improved payload capability relative to a solid propellant booster. Size optimization and fuel safety considerations resulted in a 4.57M (180 inch) diameter large booster with an inert hydrocarbon fuel. The preferred diameter for the quarter thrust level booster is 2.53M (96 inches). As part of the design study critical technology issues were identified and a technology acquistion and demonstration plan was formulated. The demonstration plan would culminate with test firings of a 3.05M (120 inch) diameter hybrid booster.

17. Key Words (Suggested by Author(s))	18. Distribution Statement
Hybrid booster, solid fuel, fuel regression, sizing study, oxidizer feed systems, test program, technology requirements.	Unclassified-unlimited

19. Security Classif. (of this report)	20. Security Classif. (of this page)	21. No. of pages	22. Price
Unclassified	Unclassified		

NASA FORM 1626 OCT 86